

ABSTRACT

interference potential due to the walls of the tunnel. The interference potential is used to obtain the upwash and the streamline curvature in the transformed plane. This is inverted to obtain the upwash and the streamline curvature in the physical plane.

WALL INTERFERENCE IN A SUBSONIC WINDTUNNEL

WITH SLOTTED WALLS

Vinay Singh

Master of Science in Engineering

Youngstown State University, 1979

A method for the calculation of wall interference in a subsonic wind-tunnel was developed. A rectangular windtunnel with slotted and solid wall elements was used. A lifting model, represented by horse shoe vortices, was placed symmetrically about the center inside windtunnel.

The total velocity potential for the flow inside the windtunnel is expressed as the summation of perturbation potential and the velocity potential at free stream velocity. The perturbation potential is the contribution from the model and the boundaries of the windtunnel. The model potential is assumed known and the interference potential, which is due to the walls of the tunnel, is calculated.

A non-dimensional Laplace equation for the interference potential is fourier transformed and solved. The particular solution is a Bessel function. This solution is used to obtain an expression for the interference potential due to any slotted or solid wall element. The expression is multiplied by the influence coefficient of each element. The influence coefficients are obtained by satisfying the boundary conditions. The total interference potential due to each element is calculated. The sum of the contribution due to all elements gives us the

interference potential due to the wall. The interference potential is used to obtain the upwash and the streamline curvature in the transformed plane. This is inverted to obtain the upwash and the streamline curvature in the physical plane.

grant number NCA2 - DP 890 701. Dr. Edwin R. Pejack was in charge of the project at Youngstown State University

The author would like to thank Dr. E. Pejack for his guidance on this project. I would also like to thank Mr. Frank Steinle for making it possible for me to spend some time at Ames-NASA.

ACKNOWLEDGEMENTS

Funding for this research was provided by NASA - Ames University Consortium under the grant number NCA2 - OR 890 701. Dr. Edwin R. Pejack was in charge of the project at Youngstown State University.

The author would like to thank Dr. E. Pejack for his guidance on this project. I would also like to thank Mr. Frank Steinle for making it possible for me to spend some time at Ames-NASA.

	PAGE
I. INTRODUCTION	1
Statement of the Problem	1
Purpose of the Study	1
Related Studies in the Field	1
II. WINDTUNNELS	4
History	4
Types of Windtunnels	5
III. WALL INTERFERENCE	10
Blockage Interference	10
Streamline Curvature	15
Upwash	15
IV. METHOD	17
Laplace Equation for the Interference Potential	19
Fourier Transformation	20
General Solution	21
Determination of Upwash	24
Determination of Streamline Curvature	27
V. INFLUENCE COEFFICIENTS	29
Boundary Condition for Slotted Wall	29

TABLE OF CONTENTS

	PAGE
ABSTRACT	ii
ACKNOWLEDGEMENT	iv
TABLE OF CONTENTS	v
LIST OF SYMBOLS	vii
LIST OF FIGURES	xi
CHAPTER	
I. INTRODUCTION	1
Statement of the Problem	1
Purpose of the Study	1
Related Studies in the Field	1
II. WINDTUNNELS	4
History	4
Types of Windtunnels	5
III. WALL INTERFERENCE	10
Blockage Interference	10
Streamline Curvature	15
Upwash	15
IV. METHOD	17
Laplace Equation for the Interference Potential	19
Fourier Transformation	20
General Solution	21
Determination of Upwash	24
Determination of Streamline Curvature	27
V. INFLUENCE COEFFICIENTS	29
Boundary Condition for Slotted Wall	29

LIST OF SYMBOLS		PAGE
SYMBOL	DEFINITION	UNITS OR REFERENCE
	Boundary Condition for Solid Wall	32
	System of Equations Used to Solve for the Influence Coefficients	34
VI.	SUMMARY	40
	Results	40
	Conclusions	42
	Recommendations	42
APPENDIX A.	Solution for the Total Interference Potential	44
APPENDIX B.	Determination of the Derivatives of the Total Interference Potential	56
APPENDIX C.	Determination of the Transform of the Velocity Potential and Its Derivatives	70
APPENDIX C.	Matrix Expressions	78
BIBLIOGRAPHY	92

h	Half of the windtunnel height	none
I_1	Interference potential of an element located at $y = \pm l$, when multiplied by the influence coefficient of the element	See Eq. (A-3)
I_2	Interference potential of an element located at $z = \pm h/s$ when multiplied by its influence coefficient	See Eq. (A-33)
I_3	y derivative of I_1	See Eq. (B-2)
I_4	z derivative of I_1	See Eq. (B-29)
I_5	z derivative of I_2	See Eq. (B-39)
I_6	y derivative of I_2	See Eq. (B-44)
$J_0(r)$	Modified Bessel function of the first kind of order ν with argument r	none
K	Constant depending upon the location of the wall element	none

LIST OF SYMBOLS

SYMBOL	DEFINITION	UNITS OR REFERENCE
a	Distance from the center of the wind-tunnel to the side walls	+ 1 for wall at $y = 1$ - 1 for wall at $y = -1$
b	Half of the windtunnel width	none
C_1, C_2	Expressions used for convenience	See Eq. (C-16) and Eq. (C-17)
e	Distance from the center of the wind-tunnel to the top and the bottom wall	+ $\frac{h}{b}$ for wall at $z = \frac{h}{b}$ - $\frac{h}{b}$ for wall at $z = -\frac{h}{b}$
F_1	Solution of I_3	See Eq. (B-13) and Eq. (B-14)
F_2	Solution of I_4	See Eq. (B-35) and Eq. (B-36)
G	Solution of I_1	See Eq. (A-20) and Eq. (A-23)
h	Half of the windtunnel height	none
I_1	Interference potential of an element located at $y = \pm 1$, when multiplied by the influence coefficient of the element	See Eq. (A-3)
I_2	Interference potential of an element located at $z = \pm h/b$ when multiplied by its influence coefficient	See Eq. (A-33)
I_3	y derivative of I_1	See Eq. (B-2)
I_4	z derivative of I_1	See Eq. (B-29)
I_5	z derivative of I_2	See Eq. (B-39)
I_6	y derivative of I_2	See Eq. (B-44)
$I_\nu(r)$	Modified Bessel function of the first kind of order ν with argument r	none
K	Constant depending upon the location of the wall element	none

K_0	Modified Bessel function of order zero	none
K_1	Number of wall elements on $0 < z < \frac{h}{b}$	See Fig. (6)
K_2	Number of wall elements on $0 < y \leq 1$ plus K_1	See Fig. (6)
$K_\nu(r)$	Modified Bessel function of 2 nd kind and of order ν with argument r	none
l	Lower limit of integration	none
M	Mach number	none
M_{1R}	Real part of the transformed model potential $(\bar{\Phi}_m)_j$	See Eq. (C-19)
M_{1i}	Imaginary part of the transformed model potential $(\bar{\Phi}_m)_j$	See Eq. (C-19)
M_{2R}	y derivative of M_{1R}	See Eq. (C-21)
M_{2i}	y derivative of M_{1i}	See Eq. (C-23)
M_{3R}	z derivative of M_{1R}	See Eq. (C-26)
M_{3i}	z derivative of M_{2i}	See Eq. (C-28)
n	As Subscript, refers to the n^{th} wall element; Normal Coordinate	none
P_1	Summation in the transformed plane of the interference potential of all wall elements	See Eq. (31) and Eq. (32)
P_1'	Function P_1 at $\sigma = \sigma'$	See Eq. (33)
P_1''	Function P_1 at $\sigma = \sigma''$	See Eq. (34)
ΔP	Pressure differences across the wall	Force/(Length) ²
q	Fourier transform variable	none
R	Porosity parameter	none
r	Radial distance of field point from center of windtunnel	Length
r'	Distance from field point to wall element	See Fig. (5)
S	Half span of the lifting model	none

u	Upper limit of integration	none
U_{∞}	Free stream velocity	Length/time
W_1	Spatial Coordinate	See Eq. (B-50)
W_2	Compressibility factor	See Eq. (B-55)
W_3	Total interference potential of an element located at $y = 1$, $0 < z < h/b$	See Eq. (A-41)
W_4	Total interference potential of an element located at $z = h/b$, $0 < y < 1$	See Eq. (A-45)
W_i	Total upwash	Length/time
x'	Normalized X	See Eq. (C-4)
X	Spatial Coordinate	Length
y', y''	Normalized Y	See Eq. (C-4)
Y	Spatial Coordinate	Length
y_j	y coordinate of the lifting element j	none
y_k	Lower limit of the element k on the wall at $z = \pm \frac{h}{b}$	Length
y_{k+1}	Upper limit of the element k on the wall at $z = \pm \frac{h}{b}$	Length
\bar{y}_n	Center of the n^{th} wall element on $z = \pm \frac{h}{b}$	Length
Δy_j	Normalized span of the lifting element j	See Eq. (C-4)
ΔY_j	Span of the lifting element j	none
z	Normalized Z	See Eq. (C-4)
z_k	Lower limit of the element k on the wall at $y = \pm 1$	Length
z_{k+1}	Upper limit of the element k on the wall at $y = \pm 1$	Length
\bar{z}_n	Center of the n^{th} wall element on wall $y = 1$	Length

Δz	Difference between upper and the lower limits of an element at $y = 1$	Length	
Z	Spatial Coordinate	Length	PAGE
β	Compressibility factor	none	11
γ_j	Normalized Γ_j	See Eq. (C-4)	13
Γ	Circulation	none	14
Γ_j	Circulation on j^{th} lifting element	none	18
δ	Distance between the wall at $y = 1$ and the	See Eq. (B-5)	23
δ	Delta function	none	27
ϵ	System for numbering wall elements	See Eq. (B-5)	30
ζ	Variable of integration $0 < z < h/b$	none	30
σ	Influence Coefficient $h/b, 0 < y < 1$	none	41
σ'	Real part of the influence coefficient	none	52
σ''	Imaginary part of the influence coefficient	none	54
σ_k	Unknown influence coefficient for the k^{th} wall element	none	71
Φ	Velocity potential	none	
Φ_i	Interference potential	none	
ϕ_i	Normalized interference potential	See Eq. (20)	
$\bar{\phi}_i$	Interference potential in the transformed plane	none	
Φ_m	Contribution of the model to the total velocity potential	none	
$(\phi_m)_j$	Normalized model potential for lifting element pair j	none	
$(\phi_{m1})_j$	x independent part of $(\phi_m)_j$	none	
$(\phi_{m2})_j$	x dependent part of $(\phi_m)_j$	none	
Ψ	Summation of C_1 and C_2	See Eq. (44)	

LIST OF FIGURES

FIGURE	CHAPTER I	PAGE
1.	Solid Blockage in a Closed Windtunnel	11
2.	Comparison of Streamlines Between Free Flight and Closed Windtunnel	13
3.	Wake Blockage in a Closed Windtunnel	14
4.	Cross Section of a Windtunnel	18
5.	Distance Between the Wall at $y = 1$ and the Field Point	23
6.	System for Numbering Wall Elements	27
7.	Wall Located at $y = 1, 0 < z < h/b$	30
8.	Wall Located at $z = h/b, 0 < y < 1$	30
9.	Arrangement of the Wall Elements for the Test Case	41
10.	Element Located at $y = 1, 0 < z < h/b$	52
11.	Element Located at $z = \frac{h}{b}, 0 < y < 1$	54
12.	Location of the Lifting Element	71

CHAPTER I

INTRODUCTION

Windtunnels are used extensively to obtain information regarding lift, drag, center of pressure etc. In order for the data to be accurate it is important that free-air conditions are duplicated while testing the model in the windtunnel. To simulate free air conditions corrections for wall interferences must be used. This thesis consists of a method to determine wall interference in a slotted wall subsonic windtunnel.

In earlier years of the development of windtunnel mostly solid wall wind tunnels were used. The size of the model tested, was usually 1% or less in size as compared to the test section area, to avoid the problem of blockage. In recent years it has become necessary to test large scale models with unprecedented accuracy. Ventilated windtunnels avoid the problem of blockage and full size models could be tested in them. Several studies have been conducted to determine the effect of the various parameters on the types of interferences for ventilated wall windtunnels. Different types of interferences may be classified as solid blockage, wake blockage, lift interference or upwash and the streamline curvature. Pindzola and Lo [9] have studied interferences in circular, two dimensional, and rectangular windtunnels with completely solid, completely open, slotted and perforated boundaries.

A basic difficulty in obtaining the wall interference corrections is in determining the correct boundary conditions. In earlier developments, the correct wall loss characteristics for porous

walls could not be determined for use in the boundary conditions. Hence, a linear wall loss characteristic was assumed [Ref (1)]. Several studies conducted later [Ref (3), (7)] showed how the boundary conditions for the slotted wall windtunnel can be obtained. It was noted that the normal velocity component for the slotted wall windtunnel would be zero at the solid portions of the wall. Across the open portions the local static pressure must be constant and equal to the upstream ambient static pressure. Initially no effect of viscosity in the flow through the slots was taken into account. Later, Baldwin, Turner and Knechtel [3] and Wood [11] derived boundary conditions where the viscous loss effect was taken into consideration. Later the boundary conditions were derived with a new concept. It was assumed that the real slotted wall could be replaced by an equivalent homogeneous boundary whose influence near the model would be very similar to that of the real wall. Several other investigators [Ref (5) (11), (10), (8)] have derived boundary conditions for equivalent wall by using different methods.

Another problem in finding the interferences is the proper representation of the model. In most previous investigations the model was mathematically simulated by placing a velocity potential singularity in the center of the tunnel. The inviscid flow field induced by the walls was then calculated, subject to the satisfaction of the wall boundary conditions. In recent years several investigators, [Ref. Davis and Moore (4), Holder (5), Wright and Bager (12), Kraft (6)] have presented results for finite span models.

In this thesis, the upwash and the streamline curvature are determined for a slotted wall rectangular windtunnel. The model was

represented by a finite set of horseshoe **vortices** along the span. The procedure used to obtain upwash and the streamline curvature is discussed in the following chapters. The thesis is mathematical in nature and most of the work is shown in the appendices.

The history of the windtunnels and their types are discussed in this chapter. The boundary conditions for each type of windtunnel are also discussed.

History

Wind tunnels have been used for the simulation of data for free flight since the beginning of this century. Wright Brothers used a crude model of a windtunnel. Since their invention, attempt has been made to produce windtunnels with more uniform flow, less turbulence and more precise measuring equipment so that the information obtained may be used to produce aerodynamically clean aircrafts.

The aircrafts tested upto 1930's had a Mach number of less than 0.5. In late 1930's it became necessary to construct windtunnels in which aircrafts of higher speeds could be tested. These aircrafts were still subsonic. Drastic changes in measurements were observed at a Mach number more than 0.6 since the density of air changes appreciably at such high speeds. This led to the possibility of developing open jet windtunnels.

In late 1930's windtunnels with slotted walls were tested. It was observed that the velocity correction is reduced by using slotted wall windtunnels. Supersonic speeds were obtained in the slotted wall wind tunnels without any choking. For subsonic testing, these windtunnels are used even today. At supersonic speeds, shockwaves developed in the slotted wall windtunnels and hence the result obtained was in error.

CHAPTER II

WIND TUNNELS

The history of the windtunnels and their types are discussed in this chapter. The boundary conditions for each type of windtunnel are also discussed.

History

Wind tunnels have been used for the simulation of data for free flight since the beginning of this century. Wright Brothers used a crude model of a windtunnel. Since their invention, attempt has been made to produce windtunnels with more uniform flow, less turbulence and more precise measuring equipment so that the information obtained may be used to produce aerodynamically clean aircrafts. The aircrafts tested upto 1930's had a Mach number of less than 0.5. In late 1930's it became necessary to construct windtunnels in which aircrafts of higher speeds could be tested. These aircrafts were still subsonic. Drastic changes in measurements were observed at a Mach number more than 0.6 since the density of air changes appreciably at such high speeds. This led to the possibility of developing open jet windtunnels.

In late 1930's windtunnels with slotted walls were tested. It was observed that the velocity correction is reduced by using slotted wall windtunnels. Supersonic speeds were obtained in the slotted wall wind tunnels without any choking. For subsonic testing, these windtunnels are used even today. At supersonic speeds, shockwaves developed in the slotted wall windtunnels and hence the result obtained was in error.

In 1950's perforated wall windtunnels were introduced which were able to cancel the shockwaves over a considerable range of Mach number. The hole size in perforated wall windtunnels should be approximately equal or larger than the thickness of the boundary layer for effectively canceling the shockwaves. To minimize the hole size the boundary layers were thinned by suction into the plenum chamber. The perforated wall windtunnels have been greatly modified since their invention and are used even today for supersonic range testing.

Types of Windtunnels

Windtunnels are basically classified as Open circuit windtunnels and Closed circuit windtunnels. In open circuit windtunnels there is no guided return of the air and the tunnel draws fresh air from the atmosphere. In closed circuit windtunnels the air is recirculated. Windtunnels are often also identified by their crosssectional shape. The classification used in this chapter is such that boundary conditions may be discussed. The three types of windtunnels classified here, are:

- 1) Open Jet Windtunnels
- 2) Closed Wind tunnels
- 3) Ventilated Windtunnels

Open Jet Windtunnel

In an open jet windtunnel there is a free jet which is surrounded by a plenum chamber at a static pressure. The pressure along the free jet boundary is also constant and equal to the undisturbed pressure upstream of the model. In equation form this can be written as:

$$P - P_{\infty} = \Delta P = 0 \quad (1)$$

where, P is the pressure at the boundary of the free jet and P_{∞} is pressure upstream of the model. In terms of velocity, the equation can be written as,

$$V_x - V_{\infty} = \Delta V_x = 0 \quad (2)$$

where, V_x : velocity at the jet boundary in x direction

V_{∞} : undisturbed free stream velocity.

The velocity potential, Φ , of any flow can be divided into,

(a) Velocity potential, ϕ_{∞} , due to the free stream velocity and (b) Velocity potential, ϕ , due to the changes in velocity. At the boundary of an open jet we get,

$$\Delta V_x = \frac{\partial \phi}{\partial x} = 0 \quad (3)$$

Hence, the above equation gives us the boundary condition for an open jet windtunnel.

Closed Windtunnels

In a closed windtunnel there are solid walls through which there can be no flow. Hence, the velocity component normal to the wall is zero. The boundary condition for a closed windtunnel is given by:

$$\frac{\partial \phi}{\partial n} = 0 \quad (4)$$

where, n - is the direction normal to the wall

and ϕ - the velocity potential due to the change in the velocity

Ventilated Windtunnels

The interferences obtained in an open jet windtunnel and a closed wall windtunnel give results with opposite signs. Ventilated wall were introduced to take advantage of this and obtain windtunnels with less interference. Not only the interference was minimized it also functioned at speeds which choked in closed windtunnels. This

enabled the use of larger models. Walls can be ventilated by making slots normal to y , z or both directions, as well as by perforations.

For boundary conditions in a slotted windtunnel the wall is often assumed at a distance different from its actual one and a homogeneous boundary condition is obtained. This equation applies along the entire length of the tunnel and for subsonic flow it is given by,

$$\frac{\partial \phi}{\partial x} + \kappa \frac{\partial^2 \phi}{\partial x \partial n} = 0 \quad (5)$$

where,

$$\kappa = \frac{\alpha}{\pi} \log_e \operatorname{Cosec} \frac{\pi a}{2d} \quad (6)$$

and has the dimensions of length.

Equation (5) was derived for inviscid flow [Ref 9] and has been corrected since then. The average boundary condition [Ref (1)] for a porous wall is derived by assuming the average velocity normal to the wall as being proportional to the pressure drop across it. This gives the boundary equation at the wall as,

$$\frac{\partial \phi}{\partial x} + \frac{1}{R} \frac{\partial \phi}{\partial n} = 0 \quad (7)$$

In the above equation R is the porosity parameter and is defined by,

$$R = \frac{fV}{\Delta P} \frac{\partial \phi}{\partial n} \quad (8)$$

where, ΔP = the pressure drop through the wall

f = the stream density

V = the stream velocity

Combining equations (5) and (7) we get a boundary equation for a slotted wall windtunnel with viscous effects within the slots. The equation is given by,

$$\frac{\partial \phi}{\partial x} + \kappa \frac{\partial^2 \phi}{\partial x \partial n} + \frac{1}{R} \frac{\partial \phi}{\partial n} = 0 \quad (9)$$

The last term in equation (9) is due to the viscous effects and it goes to zero when $R \rightarrow \infty$. Such walls are known as ideal slotted walls. When $K \rightarrow \infty$ or $R = 0$ we get $\frac{\partial \phi}{\partial n} = 0$ from equation (9) which is a special case for closed walls. For $K = 0$ and $R \rightarrow \infty$ we get $\frac{\partial \phi}{\partial x} = 0$, which is the boundary condition for open jet. (13)

For circular tunnel equation (9) reduces to,

$$\left(\frac{\partial \phi}{\partial x} + K \frac{\partial^2 \phi}{\partial x \partial r} + \frac{1}{R} \frac{\partial \phi}{\partial r} \right)_{r=R_0} \equiv 0 \quad (10)$$

where, x = free stream direction

r = cylindrical coordinate perpendicular to x

and R_0 = radius of the tunnel.

The special cases for closed, ideal and open jet circular wind-tunnel can be obtained from equation (10) by varying K and R as was done previously.

The difference between slotted and perforated wall windtunnels is in the number of openings. Perforated walls consist of numerous openings making it extremely difficult to find the interference due to each solid or slotted element. Hence a fictitious homogeneous wall is assumed to find the boundary conditions. A uniform pressure change across the wall is assumed which for the homogeneous wall is approximately given by,

$$\Delta P_{\text{wall}} = q_d K \theta \quad (11)$$

where, q_d = dynamic pressure of the flow

θ = angle between the flow and the wall

and K = constant depending upon geometry of the wall and mach number.

For the boundary condition of perforated wall the pressure drop across the wall should be equal and opposite to the change in

pressure due to the model.

Hence,

$$\Delta P_{\text{model}} + \Delta P_{\text{wall}} = 0 \quad (12)$$

In terms of velocity potential this can be written as,

$$\frac{\partial \phi}{\partial x} + \frac{1}{2} K \frac{\partial \phi}{\partial n} = 0 \quad (13)$$

The equation derived by Baldwin [Ref 3] is similar to equation (13), but it is derived in terms of porosity parameter. This equation is,

$$\frac{\partial \phi}{\partial x} + \frac{1}{R} \frac{\partial \phi}{\partial n} = 0 \quad (14)$$

When $R = 0$, we obtain the special case of closed wall. Equation (14) can be obtained from equation (9) for $K = 0$.

Perforated walls do not match the disturbances that occur in free flight as well as the slotted walls, for subsonic flow. Hence they are never used for subsonic testing.

Blockage interferences can be divided into two parts. These parts are,

- 1) Solid Blockage, caused by the presence of the model in the windtunnel.
- 2) Wake Blockage, the blockage due to the wake of the model.

Solid Blockage

The presence of the model inside a windtunnel reduces the area through which the flow must pass. The reduction in area changes the flow velocity above the model. This change in velocity due to the model is known as 'Solid Blockage'.

Fig. 1 shows 'Solid Blockage' in a closed windtunnel. The

CHAPTER III

WALL INTERFERENCE

To obtain data for a free flight condition, we must account for the interferences in the data taken in a windtunnel. Interference may arise due to the walls of the windtunnel, presence of measuring equipment and model support, and due to the unsteadiness or small scale turbulence of the flow. We are mainly concerned here with the wall interference. The wall interference can be divided into three parts.

- 1) Blockage interference
- 2) Streamline curvature
- 3) Upwash

Blockage Interference

Blockage interference can be divided into two parts. These parts are,

- 1) Solid Blockage, caused by the presence of the model in the windtunnel.
- 2) Wake Blockage, the blockage due to the wake of the model.

Solid Blockage

The presence of the model inside a windtunnel reduces the area through which the flow must pass. The reduction in area changes the flow velocity above the model. This change in velocity due to the model is known as 'Solid Blockage'.

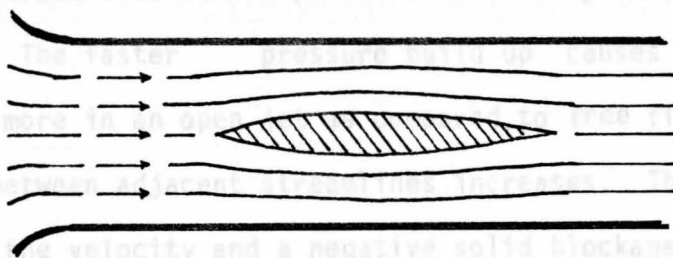
Fig. 1 shows 'Solid Blockage' in a closed windtunnel. The

velocity of the flow increases above the model due to the reduction in area through which the flow must pass. A positive solid blockage factor is obtained in a closed windtunnel.

In a free flight, the undisturbed pressure is attained after an infinite lateral distance. In an open jet (fig. 2A) this pressure build up between the model and jet boundary occurs considerably faster.

This is due to the fact that in an open jet the pressure along the free jet boundary is constant and equal to the pressure upstream of the model in an undisturbed free jet. Hence, in an open jet the undisturbed free stream pressure is already established at a finite distance.

The faster pressure build up causes the streamlines to bulge out more in an open jet in free flight. Consequently, the area between adjacent streamlines increases. This results in a decrease in the velocity and a negative solid blockage factor for an open jet windtunnel.



The development of ventilated wall wind tunnel was the result of the opposite sign interference obtained for solid wall and open jet windtunnels. The subsequent attainment of transonic test speed was merely a coincidence.

Wake Blockage

Whenever there is flow over an object, a distinct region of high turbulence and low pressure develops behind it. This region, known as wake, is caused by the separation of boundary layer.

Figure 3 shows the wake blockage in a closed windtunnel. The velocity of the fluid in the wake region is less than its velocity upstream of the model. This increases the velocity between the wall and

Fig. 1. Solid Blockage in a Closed Tunnel.

velocity of the flow increases above the model due to the reduction in area through which the flow must pass. A positive solid blockage factor is obtained in a closed windtunnel.

In a free flight, the undisturbed pressure is attained after an infinite lateral distance. In an open jet [fig. 2A] this pressure build up between the model and jet boundary occurs considerably faster.

This is due to the fact that in an open jet the pressure along the free jet boundary is constant and equal to the pressure upstream of the model in an undisturbed free jet. Hence, in an open jet the undisturbed free stream pressure is already established at a finite distance. The faster pressure build up causes the streamlines to bulge out more in an open jet as compared to free flight. Consequently, the area between adjacent streamlines increases. This results in a decrease in the velocity and a negative solid blockage factor for an open jet windtunnel.

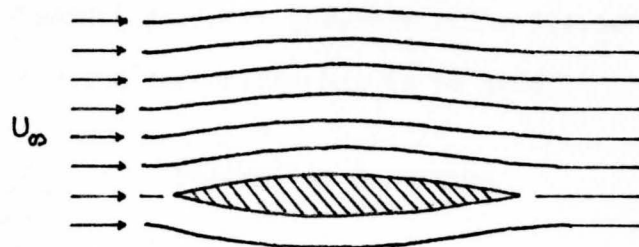
The development of ventilated wall wind tunnel was the result of the opposite sign interference obtained for solid wall and open jet windtunnels. The subsequent attainment of transonic test speed was merely a coincidence.

B. Closed Tunnel

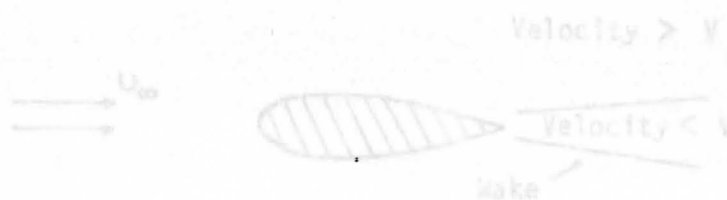
Wake Blockage

Whenever there is flow over an object, a distinct region of high turbulence and low pressure develops behind it. This region, known as wake, is caused by the separation of boundary layer.

Figure 3 shows the wake blockage in a closed windtunnel. The velocity of the fluid in the wake region is less than its velocity upstream of the model. This increases the velocity between the wall and



A. Free Flight



B. Closed Tunnel

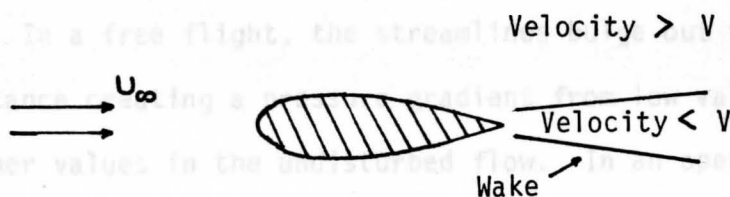
Fig. 2. Comparison Between Streamlines in a Free Flight and a Closed Windtunnel.

wake boundary to satisfy the continuity equation. The change in the flow velocity due to the presence of the wake is known as wake blockage.

The higher velocity also induces lowered pressure, which imposes a longitudinal pressure gradient. The pressure gradient induces a drag force for which correction has to be made.

Streamline Curvature

The streamlines in a free flight, open jet windtunnel and a closed wall windtunnel are shown in figure 3. The curvature of the streamlines in the three cases are different due to different boundary conditions. In a free flight, the streamlines are straight to an infinite lateral distance. In an open jet windtunnel, the streamlines are curved near the surface to higher values in the undisturbed flow. In a closed wall windtunnel the streamlines are straight near the wall.



compared to the curvatures in a free flight. The change in the streamline curvature results in a steeper pressure gradient in an open jet windtunnel. In a closed wall windtunnel the streamline curvature is reduced due to the presence of the wall where the streamline must be straight. Hence the pressure gradient in a closed wall windtunnel is less as compared to the free flight. This shows that the streamline curvature obtained in a windtunnel is different from the streamline curvature obtained in a free flight and a correction should be made to the windtunnel data.

Upwash

The upward velocity component in the wake of the model is called upwash. The upwash velocity gives the lift to the model. This component is also called upwash.

Fig. 3. Wake Blockage in a Tunnel.

wake boundary to satisfy the continuity equation. The change in the flow velocity due to the presence of the wake is known as Wake blockage.

The higher velocity also induces lowered pressure, which imposes a longitudinal pressure gradient. The pressure gradient induces a drag force for which correction has to be made.

Streamline Curvature

The streamlines in a free flight, open jet windtunnel and a closed wall windtunnel are shown in figure 2. The curvature of the streamlines in the three cases are different due to different boundary conditions. In a free flight, the streamlines bulge out to an infinite lateral distance creating a pressure gradient from low values at the surface to higher values in the undisturbed flow. In an open jet the undisturbed pressure must be attained in a finite distance. Hence the curvature of the streamlines is much more pronounced in an open jet as compared to the curvatures in a free flight. The change in the Streamline curvature results in a steeper pressure gradient in an open jet windtunnel. In a closed wall windtunnel the Streamline curvature is reduced due to the presence of the wall where the streamline must be straight. Hence the pressure gradient in a closed wall windtunnel is less as compared to the free flight. This shows that the streamline curvature obtained in a windtunnel is different from the streamline curvature obtained in a free flight and a correction should be made to the windtunnel data.

Upwash

The component of the velocity normal to the free stream velocity gives the lift to the model. This component is also called upwash.

The lift determined in a windtunnel is not the same as in a free flight condition. The discrepancy is due to the different boundary conditions in the two cases. Hence, to simulate the free flight condition it is necessary to apply the upwash correction in the windtunnel data.

Introduction

A method of determining the upwash and the streamline curvature is discussed in this chapter. A rectangular slotted windtunnel of height $2h$ and width $2b$ is shown in figure 4. The slot width and the slot spacing of the windtunnel could be varied. A lifting model is placed symmetrically about the center inside the windtunnel. The model is represented by infinite horse shoe vortices. Since it is a lifting model, there will be circulation associated with it.

For mathematical convenience we will express the velocity potential of the horse shoe vortex into y -dependent and x -independent parts. The interference potential due to both the parts have to be determined to obtain the lift interference. To determine the interference potential, the differential equation, the boundary conditions and the velocity potentials are transformed by fourier transformation. The differential equation is given by the Laplace equation. The fourier transformation of the x -independent part of the velocity potential gives a delta function. Hence, this method is also referred to as the Delta method. The slotted and the solid segments of the windtunnel wall are divided into small elements. Since the effect of the element on the interference potential depends upon the location of the element, we represent the total interference potential as a sum due to each element. In the transformed plane, the contribution of each wall element is expressed as a function with an unknown coefficient. A set of algebraic equations

CHAPTER IV

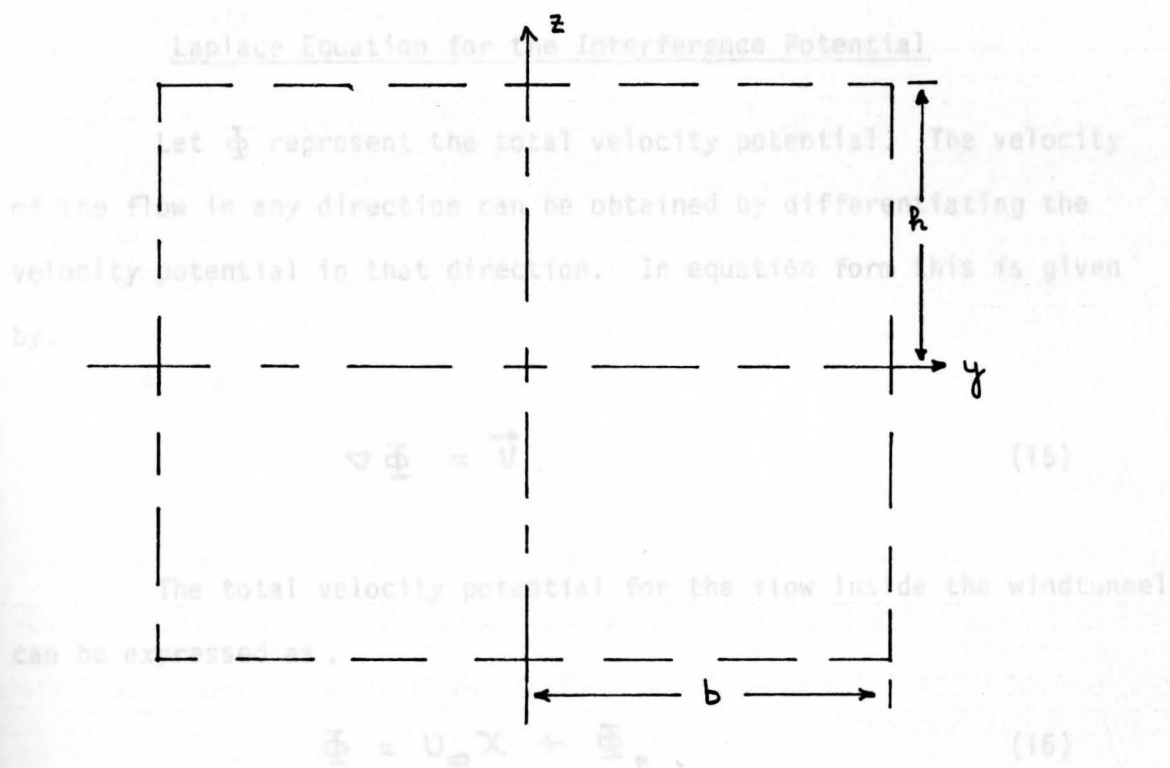
METHOD OF ANALYSIS

Introduction

A method of determining the upwash and the streamline curvature is discussed in this chapter. A rectangular slotted windtunnel of height $2h$, and width $2b$ is shown in figure 4. The slot width and the slot spacing of the windtunnel could be varied. A lifting model is placed symmetrically about the center inside the windtunnel. The model is represented by infinite horse shoe vortices. Since it is a lifting model, there will be circulation associated with it.

For mathematical convenience we will express the velocity potential of the horse shoe vortex into x -dependent and x -independent parts. The interference potential due to both the parts have to be determined to obtain the lift interference. To determine the interference potential, the differential equation, the boundary conditions and the velocity potentials are transformed by fourier transformation. The differential equation is given by the Laplace equation. The fourier transformation of the x -independent part of the velocity potential gives a delta function. Hence, this method is also referred to as the Delta method. The slotted and the solid segments of the windtunnel wall are divided into small elements. Since the effect of the element on the interference potential depends upon the location of the element, we represent the total interference potential as a sum due to each element. In the transformed plane, the contribution of each wall element is expressed as a function with an unknown coefficient. A set of algebraic equations

with these unknown coefficients is obtained by satisfying a slotted or a solid wall boundary condition at each wall element. The unknown coefficients are determined from these equations. The interference potential is now obtained by transforming back to the physical plane. Once the interference potential is known, the upwash and the streamline curvature can be obtained.



In equation (16), Φ_p is the perturbation potential. The perturbation potential is composed of, Φ_m , the contribution of the model and the interference potential, Φ_i , induced by the boundaries of the windtunnel. Hence equation (16) can be written as,

Fig. 4. Φ Cross Section of The Windtunnel (17)

The linearized form of the differential equation of a steady,

isotropic and irrotational compressible flow in terms of the velocity potential, Φ , is given by

a solid wall boundary condition at each wall element. The unknown coefficients are determined from these equations. The interference potential is now obtained by transforming back to the physical plane. Once the interference potential is known, the upwash and the streamline curvature can be obtained.

Laplace Equation for the Interference Potential

Let Φ represent the total velocity potential. The velocity of the flow in any direction can be obtained by differentiating the velocity potential in that direction. In equation form this is given by,

$$\nabla \Phi = \vec{V}. \quad (15)$$

The total velocity potential for the flow inside the windtunnel can be expressed as,

$$\Phi = U_{\infty} \chi + \Phi_p. \quad (16)$$

In equation (16), Φ_p is the perturbation potential. The perturbation potential is composed of, Φ_m , the contribution of the model and the interference potential, Φ_i , induced by the boundaries of the windtunnel. Hence equation (16) can be written as,

$$\Phi = U_{\infty} \chi + \Phi_m + \Phi_i. \quad (17)$$

The linearized form of the differential equation of a steady,

isentropic and irrotational compressible flow in terms of the velocity potential, Φ , is given by,

$$\beta^2 \frac{\partial^2 \Phi}{\partial x^2} + \frac{\partial^2 \Phi}{\partial y^2} + \frac{\partial^2 \Phi}{\partial z^2} = 0 \quad (18)$$

where, β - compressibility factor.

In normalized coordinates, equation (18) reduces to the non-dimensional Laplace equation,

$$\nabla^2 \phi = \left(\frac{\partial^2}{\partial x^2} + \frac{\partial^2}{\partial y^2} + \frac{\partial^2}{\partial z^2} \right) \phi = 0 \quad (19)$$

where,

$$x = \frac{x}{\beta b}, \quad y = \frac{y}{b}, \quad z = \frac{z}{b}, \quad \phi = \frac{\Phi}{U_\infty b} \quad (20)$$

If ϕ_m is assumed known, by representing the model by a suitable potential function, the solution of Laplace equation subject to a boundary condition on ϕ would enable us to calculate the interference potential, ϕ_i . The non-dimensional Laplace equation for the interference potential is given by,

$$\left(\frac{\partial^2}{\partial x^2} + \frac{\partial^2}{\partial y^2} + \frac{\partial^2}{\partial z^2} \right) \phi_i = 0 \quad (21)$$

Fourier Transformation

The Laplace equation for the interference potential given by equation (21) is fourier transformed according to,

$$\bar{F}(q) = \frac{1}{\sqrt{2\pi}} \int_{-\infty}^{+\infty} e^{iqx} F(x) dx \quad (22)$$

The fourier transformation of equation (21) is,

$$-q^2 \bar{\phi}_i + \left[\frac{\partial^2 \bar{\phi}_i}{\partial y^2} + \frac{\partial^2 \bar{\phi}_i}{\partial z^2} \right] = 0 \quad (23)$$

In cylindrical coordinates, equation (23) can be written as,

$$-q^2 \bar{\phi}_i + \left[\frac{\partial^2}{\partial r^2} + \frac{1}{r} \frac{\partial}{\partial r} + \frac{1}{r^2} \frac{\partial^2}{\partial \theta^2} \right] \bar{\phi}_i = 0 \quad (24)$$

When the r and θ parts of equation (24) are separated, the r part becomes a modified Bessel's equation of order m . A particular solution of equation (24) is,

$$K_0(q, r)$$

where, K_0 is a modified Bessel function of order zero.

General Solution

An approximate general solution can now be constructed by satisfying the boundary conditions at discrete points on the boundary. Interference potential is determined for each solid and slotted wall element on the tunnel boundary. The summation of the interference potential due to all the elements gives us the total interference potential.

Wall Element at $y = \pm 1$

For any general wall element k , on the wall at $y = \pm 1$, the contribution to the interference potential is,

$$(\bar{\phi}_i)_k = \sigma_k \int_{z_k}^{z_{k+1}} K_0 \left(|q| \sqrt{(z-\xi)^2 + (y-a)^2} \right) d\xi \quad (25)$$

where, $a = +1$ for the element on the wall at $y = 1$

$a = -1$ for the element on the wall at $y = -1$

$z_k =$ lower z coordinate of the k^{th} element

and $z_{k+1} =$ upper z coordinate of the k^{th} element.

The element k is divided into subelements of length $d\xi$. The argument of the modified Bessel function in equation (25) is q times the distance from each subelement to any field point. The determination of the distance is shown in figure (5). The integrated effect of the subelements times the coefficient σ_k gives the interference due to the element k . The value of σ_k has to be determined for each wall element.

Wall Element at $z = \pm \frac{h}{b}$

Similarly, for a general wall element k , on the wall $z = \pm \frac{h}{b}$ between y_k and y_{k+1} , the contribution to the interference potential is,

$$(\bar{\phi}_i)_k = \sigma_k \int_{y_k}^{y_{k+1}} K_0 \left(191 \sqrt{(z-e)^2 + (y-\xi)^2} \right) d\xi \quad (26)$$

where, $e = \frac{h}{b}$ for the wall element at $z = h/b$ and $e = -\frac{h}{b}$ for the wall element at $z = -\frac{h}{b}$.

Total Interference Potential

Equation (25) and equation (26) are evaluated in Appendix A. The value of the interference potential obtained for an element k on the wall $y = \pm 1$ is,

$$[(\phi_i)_k]_{y=\pm 1} = \sigma_k G_1 \left[191(y-a), 191(z-z_{k+1}), 191(z-z_k) \right]. \quad (27)$$

where, $a = +1$ for the wall element at $y = +1$
 $a = -1$ for the wall element at $y = -1$.

The interference potential obtained for an element k on the wall

at $z = \pm h/b$ is,

$$\phi_k(x, z) = \sigma_k \zeta \left[\frac{1}{2} \left(\frac{z - \xi}{a - y} \right) + \frac{1}{2} \left(\frac{z + \xi}{a - y} \right) \right] \quad (28)$$

where, $e = +h/b$ for the wall element at $z = h/b$

$e = -h/b$ for the wall element at $z = -h/b$

The function $G_1(z - \xi)$ is given by equation (A-23) in

Appendix A. The interference potential for any wall element can be

obtained by substituting the proper value of σ for that wall element

in equation (25) or equation (26). The value of σ for the wall element

is obtained by satisfying the boundary conditions for that element.

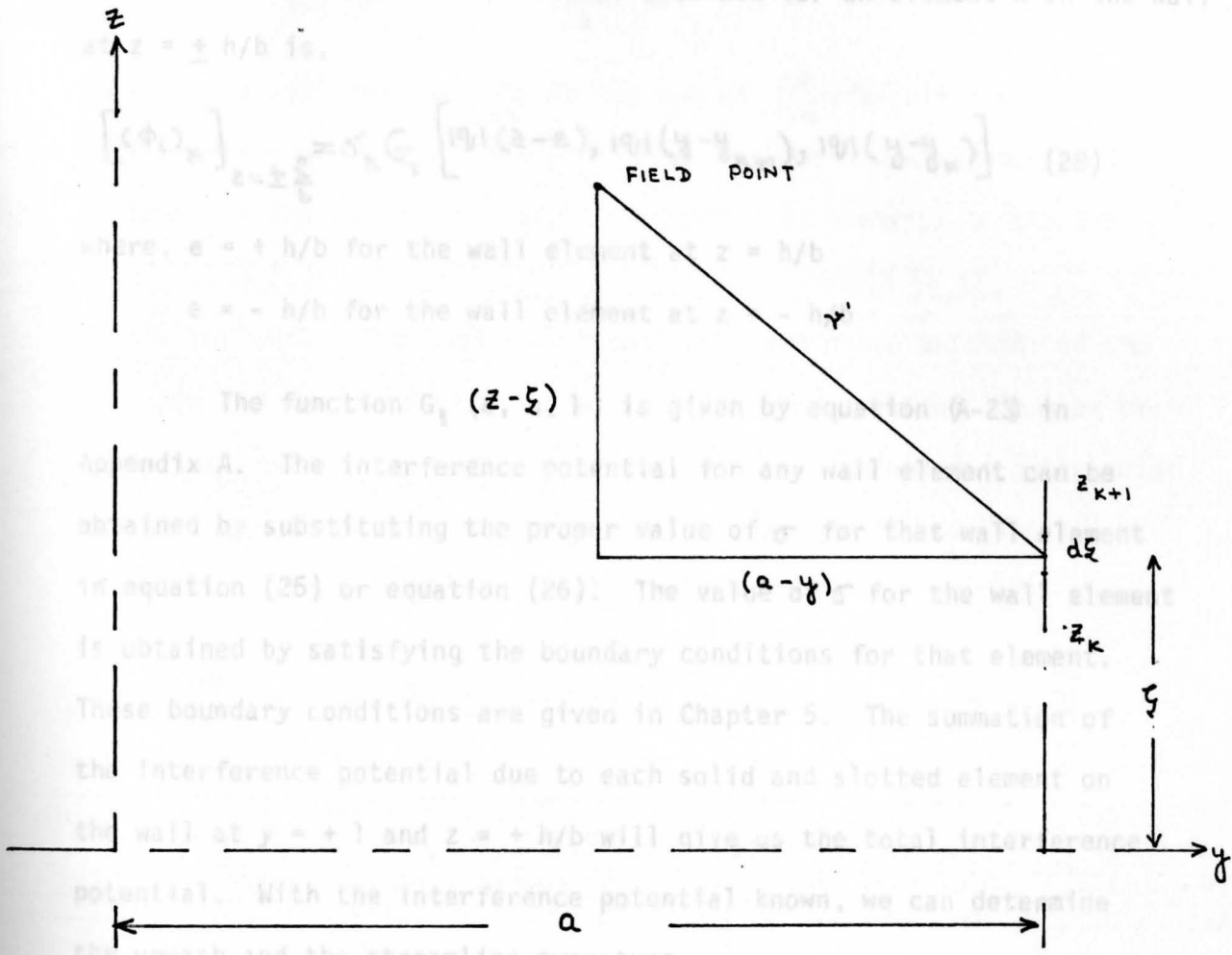
These boundary conditions are given in Chapter 5. The summation of

the interference potential due to each solid and slotted element on

the wall at $y = +1$ and $z = +h/b$ will give us the total interference

potential. With the interference potential known, we can determine

the upwash and the streamline curvature.



Determination of Upwash

The upwash can be obtained in the transformed plane by differentiating the interference potential with respect to the component z . The equation is given by,

Fig. 5. Distance Between The Wall At $y = 1$ And The Field Point

$$W_k = \frac{\partial \phi_k}{\partial z} \quad (29)$$

where, $a = +1$ for the wall element at $y = +1$

$a = -1$ for the wall element at $y = -1$.

The interference potential obtained for an element k on the wall at $z = \pm h/b$ is,

$$[\phi_i]_k \Big|_{z=\pm \frac{h}{b}} = \sigma_k G \left[191(z-e), 191(y-y_{k+1}), 191(y-y_k) \right] \quad (28)$$

where, $e = +h/b$ for the wall element at $z = h/b$

$e = -h/b$ for the wall element at $z = -h/b$

The function $G_1(\epsilon, u, l)$ is given by equation (A-23) in Appendix A. The interference potential for any wall element can be obtained by substituting the proper value of σ for that wall element in equation (25) or equation (26). The value of σ for the wall element is obtained by satisfying the boundary conditions for that element. These boundary conditions are given in Chapter 5. The summation of the interference potential due to each solid and slotted element on the wall at $y = \pm 1$ and $z = \pm h/b$ will give us the total interference potential. With the interference potential known, we can determine the upwash and the streamline curvature.

Determination of Upwash

The upwash can be obtained in the transformed plane by differentiating the interference potential with respect to the component z . The equation is given by,

$$\bar{W}_i = \frac{\partial}{\partial z} \bar{\phi}_i \quad (29)$$

The upwash in the physical plane is obtained by taking the reverse transform. Hence, the upwash in the physical plane is

$$W_i = \frac{1}{\sqrt{2\pi}} \int_{-\infty}^{+\infty} \frac{\partial \bar{\phi}_i}{\partial z} e^{-iqx} dq. \quad (30)$$

In equation (30) the term $\frac{\partial \bar{\phi}_i}{\partial z}$ is the sum of $\frac{\partial(\phi_i)_k}{\partial z}$ for all the elements on the wall $y = \pm 1$ and $z = \pm \frac{h}{b}$. Fig. 6 shows the distribution of elements on the tunnel boundary. The number of elements on the top half of the left wall is K_1 . There are $K_2 - K_1$ elements on the right half of the top wall. The number of elements on the other sections of the wall are also shown in the figure 6. The word 'section' is used here as half of the wall on any side of the tunnel. In Appendix B the total upwash is obtained by determining the contribution of each section of the wall. The equation for upwash can be written as,

$$\begin{aligned} \frac{\partial \bar{\phi}_i}{\partial z} = & \sum_{k=1}^{K_1} \sigma_k F_2 \left[\rho_1(y+1), \rho_1(z-z_{k+1}), \rho_1(z-z_k) \right] \\ & - \sum_{k=1}^{K_1} \sigma_k F_2 \left[\rho_1(y+1), \rho_1(z+z_k), \rho_1(z+z_{k+1}) \right] \\ & + \sum_{k=1}^{K_1} \sigma_k F_2 \left[\rho_1(y-1), \rho_1(z-z_{k+1}), \rho_1(z-z_k) \right] \\ & - \sum_{k=1}^{K_1} \sigma_k F_2 \left[\rho_1(y-1), \rho_1(z+z_k), \rho_1(z+z_{k+1}) \right] \\ & + \sum_{k=K_1+1}^{K_2} \sigma_k F_1 \left[\rho_1(z-\frac{h}{b}), \rho_1(y+y_k), \rho_1(y+y_{k+1}) \right] \\ & + \sum_{k=K_1+1}^{K_2} \sigma_k F_1 \left[\rho_1(z-\frac{h}{b}), \rho_1(y-y_{k+1}), \rho_1(y-y_k) \right] \end{aligned}$$

$$\begin{aligned}
& - \sum_{K=K_1+1}^{K_2} \sigma_K F_1 \left[191(z + R/b), 191(y + y_K), 191(y + y_{K+1}) \right] \\
& - \sum_{K=K_1+1}^{K_2} \sigma_K F_1 \left[191(z + R/b), 191(y - y_{K+1}), 191(y - y_K) \right] . \quad (31)
\end{aligned}$$

In equation (31) the terms are due to the contribution from the section top half of left wall, bottom half of left wall, top half of right wall, bottom half of right wall, left half of top wall, right half of top wall, left half of bottom wall and the right half of bottom wall respectively. Equation (31) is a function of q , y and z and can be written as ,

$$\frac{\partial \bar{\phi}_i}{\partial z} = P_i(q, y, z) . \quad (32)$$

If the influence coefficient, σ , has a real part, σ' and an imaginary part σ'' , then $P_i(q, y, z)$ will also have a real and an imaginary part. The real part is,

$$P_i'(q, y, z) = [P_i(q, y, z)]_{\sigma=\sigma'} . \quad (33)$$

The imaginary part is,

$$P_i''(q, y, z) = [P_i(q, y, z)]_{\sigma=\sigma''} . \quad (34)$$

Therefore, the upwash is,

$$W_i = \frac{1}{\sqrt{2\pi}} \int_{-\infty}^{+\infty} [P_i'(q, y, z) + P_i''(q, y, z)] e^{-iqx} dq . \quad (35)$$

Equation (35) can also be written as,

$$\begin{aligned}
W_i = \frac{1}{\sqrt{2\pi}} \int_{-\infty}^{+\infty} \{ & [P_i'(q, y, z) \cos qx - i P_i'(q, y, z) \sin qx] \\
& + [P_i''(q, y, z) \cos qx - i P_i''(q, y, z) \sin qx] \} dq . \quad (36)
\end{aligned}$$

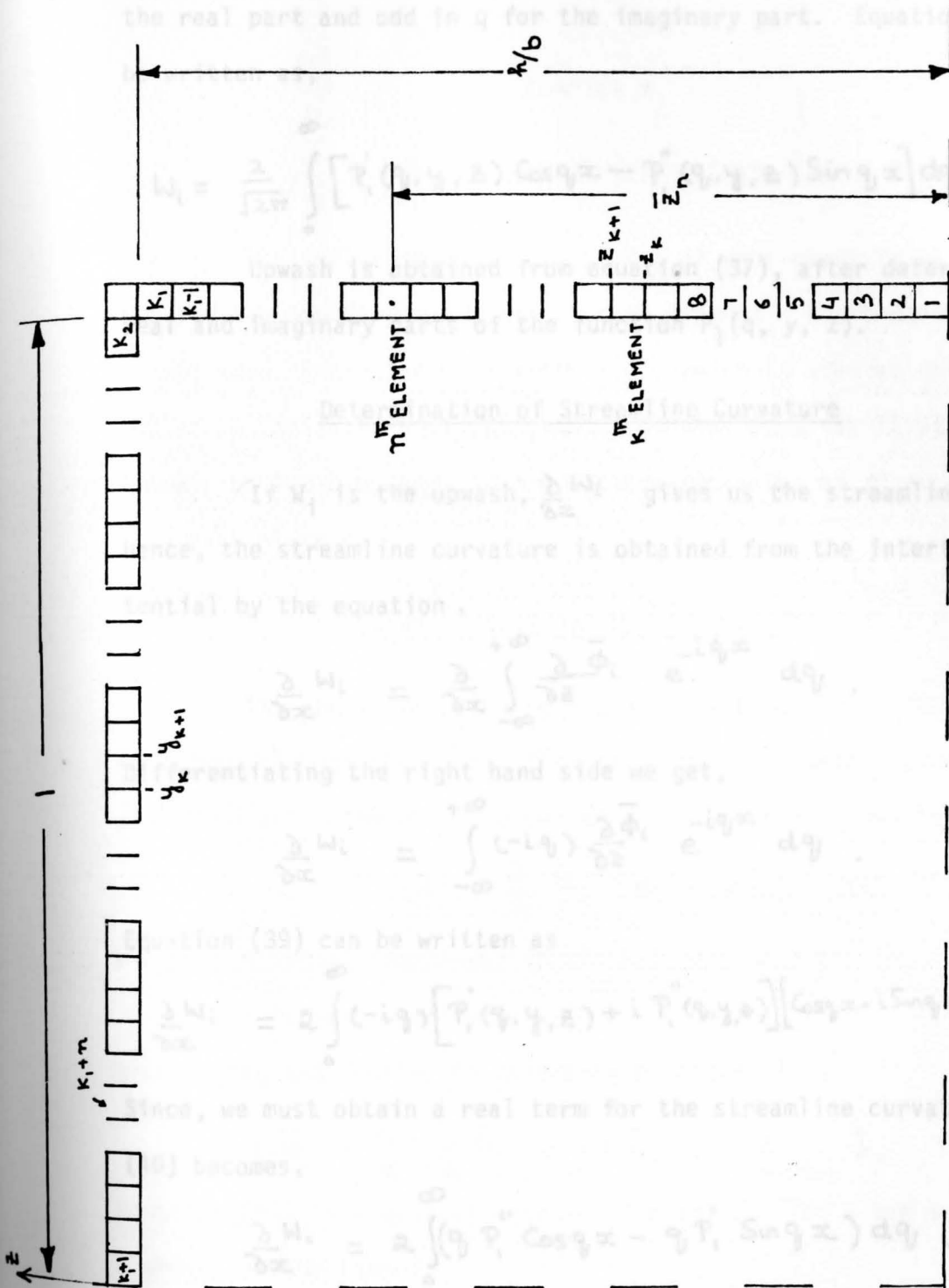


Fig. 6. System For Numbering Elements

The upwash, W_1 , is real. Hence, $\frac{\partial W_1}{\partial x}$ must be even in q for the real part and odd in q for the imaginary part. Equation (36) can now

$$W_1 = \frac{1}{2\pi} \int_0^\pi [P_1(q, y, z) \cos q x + i P_2(q, y, z) \sin q x] dq \quad (37)$$

Downwash is obtained from equation (37) after determining the real and imaginary parts of the function $P_1(q, y, z)$.

Determination of Streamline Curvature

If W_1 is the upwash, $\frac{\partial W_1}{\partial x}$ gives us the streamline curvature. Hence, the streamline curvature is obtained from the interference potential by the equation.

$$\frac{\partial^2 W_1}{\partial x^2} = \frac{\partial}{\partial x} \int_0^\pi \frac{\partial P_1}{\partial x} e^{-iqx} dq$$

Differentiating the right hand side we get.

$$\frac{\partial^2 W_1}{\partial x^2} = \int_0^\pi (-iq) \frac{\partial P_1}{\partial x} e^{-iqx} dq$$

Equation (39) can be written as

$$\frac{\partial^2 W_1}{\partial x^2} = 2 \int_0^\pi (-iq) [P_1'(q, y, z) + i P_2'(q, y, z)] [\cos qx - i \sin qx] dq$$

Since, we must obtain a real term for the streamline curvature, equation (40) becomes.

$$\frac{\partial^2 W_1}{\partial x^2} = 2 \int_0^\pi (q P_2' \cos qx - q P_1' \sin qx) dq \quad (41)$$

The above equation is used to determine the streamline curvature once the real and the imaginary parts of the function $P_1(q, y, z)$ are known.

The upwash, W_i , is real. Hence, $\frac{\partial}{\partial z} \bar{\phi}_i$ must be even in q for the real part and odd in q for the imaginary part. Equation (36) can now be written as,

$$W_i = \frac{2}{\sqrt{2\pi}} \int_0^{\infty} \left[P_1'(q, y, z) \cos qx - P_1''(q, y, z) \sin qx \right] dq. \quad (37)$$

Upwash is obtained from equation (37), after determining the real and imaginary parts of the function $P_1(q, y, z)$.

Determination of Streamline Curvature

If W_i is the upwash, $\frac{\partial W_i}{\partial x}$ gives us the streamline curvature. Hence, the streamline curvature is obtained from the interference potential by the equation,

$$\frac{\partial W_i}{\partial x} = \frac{\partial}{\partial x} \int_{-\infty}^{+\infty} \frac{\partial \bar{\phi}_i}{\partial z} e^{-iqx} dq. \quad (38)$$

Differentiating the right hand side we get,

$$\frac{\partial W_i}{\partial x} = \int_{-\infty}^{+\infty} (-iq) \frac{\partial \bar{\phi}_i}{\partial z} e^{-iqx} dq. \quad (39)$$

Equation (39) can be written as

$$\frac{\partial W_i}{\partial x} = 2 \int_0^{\infty} (-iq) \left[P_1'(q, y, z) + i P_1''(q, y, z) \right] \left[\cos qx - i \sin qx \right] dq. \quad (40)$$

Since, we must obtain a real term for the streamline curvature, equation (40) becomes,

$$\frac{\partial W_i}{\partial x} = 2 \int_0^{\infty} (q P_1'' \cos qx - q P_1' \sin qx) dq. \quad (41)$$

The above equation is used to determine the streamline curvature once the real and the imaginary parts of the function $P_1(q, y, z)$ are known.

CHAPTER V

THE INFLUENCE COEFFICIENTS

The influence coefficient, σ , of an element is obtained by satisfying the boundary condition of that element. The boundary condition is obtained, depending on whether the element is slotted or solid. The influence coefficient of the element depends upon the location of the element on the boundary. Hence a different value of σ is obtained for each wall element.

Boundary Condition For Slotted Wall

The normal velocity to the wall is proportional to the pressure drop through the slot. This leads to the boundary condition for a slotted wall element. The boundary condition is given by,

$$\left[\frac{\partial}{\partial x} + \frac{\beta}{R} \frac{\partial}{\partial n} \right] [\phi_i + \phi_m] = 0 \quad (42)$$

where, n = Normal coordinate to the wall $\pm y$ or $\pm z$

R = Porosity parameter

Rearranging and fourier transforming equation (42),

$$-i q \bar{\phi}_i + \frac{\beta}{R} \frac{\partial \bar{\phi}_i}{\partial n} = i q \bar{\phi}_m - \frac{\beta}{R} \frac{\partial \bar{\phi}_m}{\partial n} . \quad (43)$$

Equation (43) is a general equation for any slotted element on the boundary of the tunnel.

Wall Element on $y = 1, 0 < z < h/b$

Figure 7 shows the portion of the wall which is represented by $y = 1, 0 < z < h/b$. If the slotted wall element is located on this

wall, the equation for a representative n^{th} wall element is,

$$-Lq W_3(n, y) + \frac{\rho}{R} \frac{\partial}{\partial y} (W_3(n, y)) = Lq [M_{12} + (C_1 + C_2) \delta(y) + iM_{11}] - z [M_{22} + \rho \delta(y) + iM_{21}] \quad (44)$$

The value $\frac{\partial}{\partial y} W_3$ is obtained from Appendix A and of ϕ_m from Appendix C. Since, $\frac{\partial}{\partial y} W_3$ is represented by ψ from the notations used in Appendix D, equation (44) can be written as,

$$-Lq W_3(n, y) + \frac{\rho}{R} W_3(n, y) = Lq [M_{12} + (C_1 + C_2) \delta(y) + iM_{11}] - z [M_{22} + \rho \delta(y) + iM_{21}] \quad (45)$$

Expressing the complex influence coefficient as,

$$C_k = \sigma_k + i\tau_k \quad (46)$$

and letting the primes and the double primes on the functions W_1 and W_3

represent their real and imaginary parts respectively, the real part of equation (45) is,

$$-Lq W_3'(n, y) + \frac{\rho}{R} W_3'(n, y) = -Lq M_{12} - \frac{\rho}{R} M_{22} - \frac{\rho}{R} \rho \delta(y) \quad (47)$$

and the imaginary part of equation (45) is,

$$-Lq W_3''(n, y) + \frac{\rho}{R} W_3''(n, y) = Lq M_{11} - Lq (C_1 + C_2) \delta(y) \quad (48)$$

Wall Element on $z = h/b, 0 < y < 1$

Figure (8) shows the portion of the wall represented by

$z = h/b, 0 < y < 1$. Equation (4) is evaluated for a representative n^{th}

wall element on this wall. Substituting the values of $\phi_1, \frac{\partial}{\partial y} \phi_1, \bar{\phi}_m$

and $\frac{\partial}{\partial y} \bar{\phi}_m$ in equation (43) we

$$-Lq W_4(n, y) + \frac{\rho}{R} W_4(n, y) = Lq [M_{12} + iM_{11} + (C_1 + C_2) \delta(y)] - \frac{\rho}{R} [M_{22} + M_{21} L + \rho \delta(y)] \quad (49)$$

Fig. 8. Wall Located At $z = \frac{h}{b}, 0 < y < 1$

wall, the equation for a representative n^{th} wall element is,

$$-i q W_3(n, q) + \frac{\beta}{R} \frac{\partial}{\partial y} (W_3(n, q)) = i q [M_{1R} + (C_1 + C_2) \delta(q) + i M_{1i}] - \frac{\beta}{R} [M_{2R} + \xi \delta(q) + i M_{2i}] \quad (44)$$

The value of ϕ_i was obtained from Appendix A and of ϕ_m from Appendix C. Since, $\frac{\partial}{\partial y} W_3$ is represented by w_1 from the notations used in Appendix D, equation (44) can be written as,

$$-i q W_3(n, q) + \frac{\beta}{R} W_1(n, q) = i q (M_{1R} + (C_1 + C_2) \delta(q) + i M_{1i}) - \frac{\beta}{R} (M_{2R} + \xi \delta(q) + i M_{2i}) \quad (45)$$

Expressing the complex influence coefficient as,

$$\sigma_K = \sigma'_K + \sigma''_K \quad (46)$$

and letting the primes and the double primes on the functions W_1 and W_3 represent their real and imaginary parts respectively, the real part of equation (45) is,

$$q W_3''(n, q) + \frac{\beta}{R} W_1'(n, q) = -q M_{1i} - \frac{\beta}{R} M_{2R} - \frac{\beta}{R} \xi \delta(q) \quad (47)$$

and the imaginary part of equation (45) is,

$$-q W_3'(n, q) + \frac{\beta}{R} W_1''(n, q) = q M_{1R} + q (C_1 + C_2) \delta(q) - \frac{\beta}{R} M_{2i} \quad (48)$$

Wall Element on $z = h/b$, $0 < y < 1$

Figure (8) shows the portion of the wall represented by $z = h/b$, $0 < y < 1$. Equation (43) is evaluated for a representative n^{th} wall element on this wall. Substituting the values of $\bar{\phi}_i$, $\frac{\partial}{\partial n} \bar{\phi}_i$, $\bar{\phi}_m$ and $\frac{\partial}{\partial n} \bar{\phi}_m$ in equation (43) we get,

$$-i q W_4(n, q) + \frac{\beta}{R} W_2(n, q) = i q [M_{1R} + i M_{1i} + (C_1 + C_2) \delta(q)] - \frac{\beta}{R} [M_{3R} + M_{3i} i + \nu \delta(q)] \quad (49)$$

Let primes and double primes represent the real and imaginary parts of functions W_4 and W_2 . Separating the real and the imaginary parts of the equation (49);

Real part:

$$\rho W_4''(n, \rho) + \frac{\beta}{R} W_2'(n, \rho) = -\rho M_{ii} - \frac{\beta}{R} M_{3R} - \frac{\beta}{R} \nu \delta(\rho) \quad (50)$$

Imaginary part:

$$-\rho W_4'(n, \rho) + \frac{\beta}{R} W_2''(n, \rho) = \rho M_{iR} + \rho (c_1 + c_2) \delta(\rho) - \frac{\beta}{R} M_{3i} \quad (51)$$

Boundary Condition for Solid Wall

There is no flow across a solid wall element, hence the boundary condition is given by,

$$\frac{\partial}{\partial n} (\phi_i + \phi_m) = 0. \quad (52)$$

Fourier transforming equation (52),

$$\frac{\partial}{\partial n} \bar{\phi}_i = - \frac{\partial}{\partial n} \bar{\phi}_m. \quad (53)$$

Equation (53) is a general equation for any solid element on the tunnel boundary.

Wall Element on $y = 1$, $0 < z < h/b$

Figure (6) shows the position of the wall on which the element is located. In equation (53), the value of $\bar{\phi}_i$ is substituted from Appendix A and of $\bar{\phi}_m$ from Appendix C. For the n^{th} wall element equation (53) reduces to,

$$\frac{\partial}{\partial y} (\bar{\phi}_i) = - \frac{\partial}{\partial y} (M_{iR} + (c_1 + c_2) \delta(\rho) + i M_{ii}). \quad (54)$$

Using the notations from Appendix D, equation (54) can be written as,

$$W_1(n, q) = -M_{2R} - \xi \delta(q) - i M_{2i} \quad (55)$$

The real and the imaginary parts of $W_1(n, q)$ are substituted in equation (55). The real part is denoted by a prime and the double prime denotes the imaginary part. Equation (55) is then separated into the real and the imaginary parts. The real part of equation (55) is,

$$W_1'(n, q) = -M_{2R} - \xi \delta(q) \quad (56)$$

and the imaginary part is given by,

$$W_1''(n, q) = -M_{2i} \quad (57)$$

Wall Element on $z = h/b$, $0 < y < 1$

Figure (7) shows the position of the wall on which the element is located. Substituting the values of $\bar{\phi}_i$ and $\bar{\phi}_{m_1}$ equation (53) for this element can be written as,

$$W_2(n, q) = -(M_{3R} + \nu \delta(q) + i M_{3i}) \quad (58)$$

Separating the real and imaginary parts of equation (58) we get,

Real part:

$$W_2'(n, q) = -M_{3R} - \nu \delta(q) \quad (59)$$

Imaginary part:

$$W_2''(n, q) = -M_{3i} \quad (60)$$

To find the influence coefficient we have to satisfy the boundary condition equations (47), (48), (50), (51), (56), (57), (59) and (60). Appendix D defines the terms W_1 , W_2 , W_3 , W_4 , M_1 , M_3 , ξ , $(c_1 + c_2)$ and ν .

System of Equations

A set of equations is developed for all the wall elements. Each equation has a real and an imaginary part. Thus the total number of equations is twice the number of the wall elements. These equations are described below.

Slotted Wall Elements at $y = 1$

Real Part of the Equation

The real part of the boundary condition equation for the slotted wall elements located at $y = 1$ is given by equation (47). Equation (47) can be written as a matrix equation for all the $(K_1 - N_1)$ slotted elements on the wall $y = 1$ by using Appendix D. Equations (D-4), (D-17), (D-25), (D-31) and equation (D-48) are substituted in equation (47). The matrix equation thus obtained is given by,

$$\rho \{C\} \{\sigma''\} + \frac{\beta}{R} \{T\}_{y=1} \{\sigma'\} = -\rho \{M_{ii}, y\} - \frac{\beta}{R} \{M_{2R}, y\} - \frac{\beta}{R} \{Q\} \delta(\rho) \quad (61)$$

where,

$$\{M_{ii}, y\}_n = \left[M_{ii} \right]_{y=1, z=\bar{z}_n} \quad (62)$$

and

$$\{M_{2R}, y\}_n = \left[M_{2R} \right]_{y=1, z=\bar{z}_n} \quad (63)$$

The subscript n represents the index of the slotted wall elements on the wall $y = 1$. Equation (61) represents $(K_1 - N_1)$ equations with $2K_2$ unknowns for N_1 solid elements on the wall at $y = 1$.

Imaginary Part of the Equation

The imaginary part of the boundary equation for the slotted wall elements at $y = 1$ is given by equation (48). By substituting equations (D-5), (D-16), (D-28) and (D-34), we can write equation (48) in matrix form. This matrix equation is,

$$-q \{c\} \{\sigma'\} + \frac{p}{R} \{T\}_{y_{\text{slot}}} \{\sigma''\} = q \{M_{1R, y}\} - \frac{p}{R} \{M_{2i, y}\} + q \{\psi\} \delta(q) \quad (64)$$

where,

$$\{M_{1R, y}\} = [M_{1R}]_{\substack{y=1 \\ z=\bar{z}_n}} \quad (65)$$

and

$$\{M_{2i, y}\} = [M_{2i}]_{\substack{y=1 \\ z=\bar{z}_n}} \quad (66)$$

Equation (64) represents $(K_1 - N_1)$ equations with $2K_2$ unknowns.

Slotted Wall Elements at $z = h/b$

Real Part of the Equation

The real part of the boundary condition equation for a slotted wall element at $z = \frac{h}{b}$ is given by equation (50). By using equations (D-9), (D-22), (D-25) (D-37) and (D-43) we write equation (50) in matrix form for all the slotted elements on the wall $z = \frac{h}{b}$. This equation is,

$$q \{D\} \{\sigma''\} + \frac{p}{R} \{U\}_{z_{\text{slot}}} \{\sigma'\} = -q \{M_{1i, z}\} - \frac{p}{R} \{M_{3R, z}\} - \frac{p}{R} \{v\} \delta(q) \quad (67)$$

where,

$$\{M_{1i, z}\} = [M_{1i}]_{\substack{z = h/b \\ y = \bar{y}_n}} \quad (68)$$

and,

$$\{M_{3R,z}\} = [M_{3R}] \quad \begin{matrix} z = h/b \\ y = \bar{y}_n \end{matrix} \quad (69)$$

Imaginary Part of the Equation

The imaginary part of the boundary condition equation for slotted elements on the wall $z = h/b$ is given by equation (51). By using equations (D-21), (D-10), (D-28), (D-43) and (D-40) we write equation (51) into a matrix form. This matrix equation is given by,

$$-q \{D\} \{\sigma'\} + \frac{\beta}{R} \{U\}_{z=slot} \{\sigma''\} = q \{M_{1R,z}\} - \frac{\beta}{R} \{M_{3i,z}\} + q \{\psi\} \delta(q) \quad (70)$$

where,

$$\{M_{1R,z}\} = [M_{1R}] \quad \begin{matrix} z = h/b \\ y = \bar{y}_n \end{matrix} \quad (71)$$

and

$$\{M_{3i,z}\} = [M_{3i}] \quad \begin{matrix} z = h/b \\ y = \bar{y}_n \end{matrix} \quad (72)$$

Solid Elements at $y = 1$

Real Part of the Equation

The real part of the boundary condition equation for a solid element on the wall $y = 1$ is given by equation (56). Using equations (D-4), (D-31) and (D-48) we can express equation (56) by the matrix equation,

$$\{T\}_{y=solid} \{\sigma'\} = \{M_{2R,y}\} - \{\tau\} \delta(q) \quad (73)$$

Imaginary Part of the Equation

The imaginary part of the boundary condition equation for a solid wall element is given by equation (57). By using equations (D-5) and (D-34) we can express equation (57) by the matrix equation,

$$\{\tau\}_{y \text{ Solid}} \{\sigma''\} = -\{M_{2i,y}\} \quad (74)$$

Solid Elements at $z = \frac{h}{b}$

Real Part of the Equation

The real part of the boundary condition equation for a solid wall element at $z = \frac{h}{b}$ is given by equation (59). By using equations (D-9), (D-37) and (D-43) we can express equation (59) in matrix form for all the solid elements on the wall $z = \frac{h}{b}$. This matrix equation is,

$$\{u\}_{z \text{ Solid}} \{\sigma'\} = -\{M_{3R,z}\} - \{v\} \delta(\rho) \quad (75)$$

where,

$$\{M_{3R,z}\} = [M_{3R}]_{\substack{z = h/b \\ y = \bar{y}_n}} \quad (76)$$

Imaginary Part of the Equation

The imaginary part of the boundary condition equation for a solid wall element at $z = \frac{h}{b}$ is given by equation (60). By substituting equations (D-10) and (D-40) in equation (60) a matrix equation is obtained for all the solid elements at $z = \frac{h}{b}$. This equation is given by,

$$\{u\}_{z \text{ Solid}} \{\sigma''\} = -\{M_{3i,z}\} \quad (77)$$

Hence, a set of $2K_2$ equations is obtained for all the slotted

and the solid elements with $2K_2$ unknowns. The unknowns are the real and the imaginary part of the influence coefficients. These equations can be written as one matrix equation in the form,

$$\{A\} \{\sigma^{III}\} = \{M\} + \{B\} \delta(q) \quad (78)$$

The left hand side of the equation (78) is,

$$\{A\} \{\sigma^{III}\} = \begin{bmatrix} \{T\}_{Y \text{ SOLID}} & 0 \\ \{U\}_{Z \text{ SOLID}} & 0 \\ \frac{B}{R} \{T\}_{Y \text{ SLOT}} & q\{C\} \\ -q\{C\} & \frac{B}{R} \{T\}_{Y \text{ SLOT}} \\ \frac{B}{R} \{U\}_{Z \text{ SLOT}} & q\{D\} \\ -q\{D\} & \frac{B}{R} \{U\}_{Z \text{ SLOT}} \\ 0 & \{T\}_{Y \text{ SOLID}} \\ 0 & \{U\}_{Z \text{ SOLID}} \end{bmatrix} \begin{bmatrix} q_{K_1} \\ \vdots \\ q_{K_2} \\ \vdots \\ q_{K_2} \\ \vdots \\ q_{K_1} \end{bmatrix}$$

The right side of equation (78) is,

$$\begin{bmatrix} -\{M_{2R,Y}\}_{\text{SOLID}} \\ -\{M_{3R,Z}\}_{\text{SOLID}} \\ -q\{M_{1i,Y}\}_{\text{SLOT}} - \frac{B}{R} \{M_{2R,Y}\}_{\text{SLOT}} \\ q\{M_{1R,Y}\}_{\text{SLOT}} - \frac{B}{R} \{M_{2i,Y}\}_{\text{SLOT}} \\ -q\{M_{1i,Z}\}_{\text{SLOT}} - \frac{B}{R} \{M_{3R,Z}\}_{\text{SLOT}} \\ q\{M_{1R,Z}\}_{\text{SLOT}} - \frac{B}{R} \{M_{3i,Z}\}_{\text{SLOT}} \\ -\{M_{2i,Y}\}_{\text{SOLID}} \\ -\{M_{3i,Z}\}_{\text{SOLID}} \end{bmatrix} + \begin{bmatrix} -\{v\}_{Y \text{ SOLID}} \\ -\{w\}_{Z \text{ SOLID}} \\ -\frac{B}{R} \{v\}_{Y \text{ SLOT}} \\ q\{v\}_{Y \text{ SLOT}} \\ -\frac{B}{R} \{w\}_{Z \text{ SLOT}} \\ q\{w\}_{Z \text{ SLOT}} \\ 0 \\ 0 \end{bmatrix} \delta(q)$$

The matrix given by equation (78) is solved to obtain the values of the influence coefficients. Once the influence coefficients are

determined, the interference potential can be obtained by using equation (25) and equation (26).

CHAPTER VI

SUMMARY

Results

A method for the calculation of wall interference in a wind-tunnel has been presented in this thesis. Equation (37) was derived to evaluate the upwash. The streamline curvature is determined by equation (41). These equations contain unknown values of the influence coefficients of the wall elements. The influence coefficients are determined using equation (78).

A computer program was used to calculate the lift interference and the streamline curvature. The calculations were performed for one case only. Figure 9 shows the arrangement of the solid and slotted wall elements for the test case. The porosity parameter of the slotted wall element was taken as one, and the porosity parameter of the solid wall element was taken as zero. The lift was evaluated at an element located at the center of the tunnel. The upwash determined at this point was 0.1056 and the streamline curvature was 0.1825. These calculations compared favorably with the results of Pejack and Steinle,¹ and Kraft [6]. Various values of the upwash and the streamline curvature can be obtained at different locations on the wing for different tunnel size, porosity parameter and wall element sizes. This can enable us to compare the data for different variables. These calculations can be used not only in correcting the data obtained in a wind-

¹Publication pending.

CHAPTER VI

SUMMARY

Results

A method for the calculation of wall interference in a wind-tunnel has been presented in this thesis. Equation (37) was derived to evaluate the upwash. The streamline curvature is determined by equation (41). These equations contain unknown values of the influence coefficients of the wall elements. The influence coefficients are determined using equation (78).

A computer program was used to calculate the lift interference and the streamline curvature. The calculations were performed for one case only. Figure 9 shows the arrangement of the solid and slotted wall elements for the test case. The porosity parameter of the slotted wall element was taken as one, and the porosity parameter of the solid wall element was taken as zero. The lift was evaluated at an element located at the center of the tunnel. The upwash determined at this point was 0.1056 and the streamline curvature was 0.1825. These calculations compared favorably with the results of Pejack and Steinle,¹ and Kraft [6]. Various values of the upwash and the streamline curvature can be obtained at different locations on the wing for different tunnel size, porosity parameter and wall element sizes. This can enable us to compare the data for different variables. These calculations can be used not only in correcting the data obtained in a wind-

¹Publication pending.

tunnel test, but also in designing windtunnels with minimum interference.

Conclusion

Theories for predicting the interference effects in windtunnel have been available for more than 25 years. The methods used in most of the previous studies for investigating the wall interference used a homogeneous wall boundary. The homogeneous wall is an approximation with several limitations. Methods based on the homogeneous wall conditions become less exact as the lifting model span becomes larger. For large slot spacing also, the solution obtained using homogeneous wall is not very accurate. The method described in this thesis uses an exact, non-homogeneous boundary condition. A set of equations was solved to calculate the interfering influence of each small segment on the wall. Since the effect of each of these segments is different on the total interference, a much more accurate result is obtained. The variables, such as the location of the solid and the slotted elements and the porosity parameters, can be obtained by this method without any difficulty. The delta function obtained in the equations poses no problem. If the model function is divided into x -dependent and x -independent parts, the result obtained due to the delta part of the equations is the same as the result due to the x -independent part of the model potential. Hence, this method avoids the problem of splitting the problem into x -dependent and x -independent parts to obtain the total interference potential.

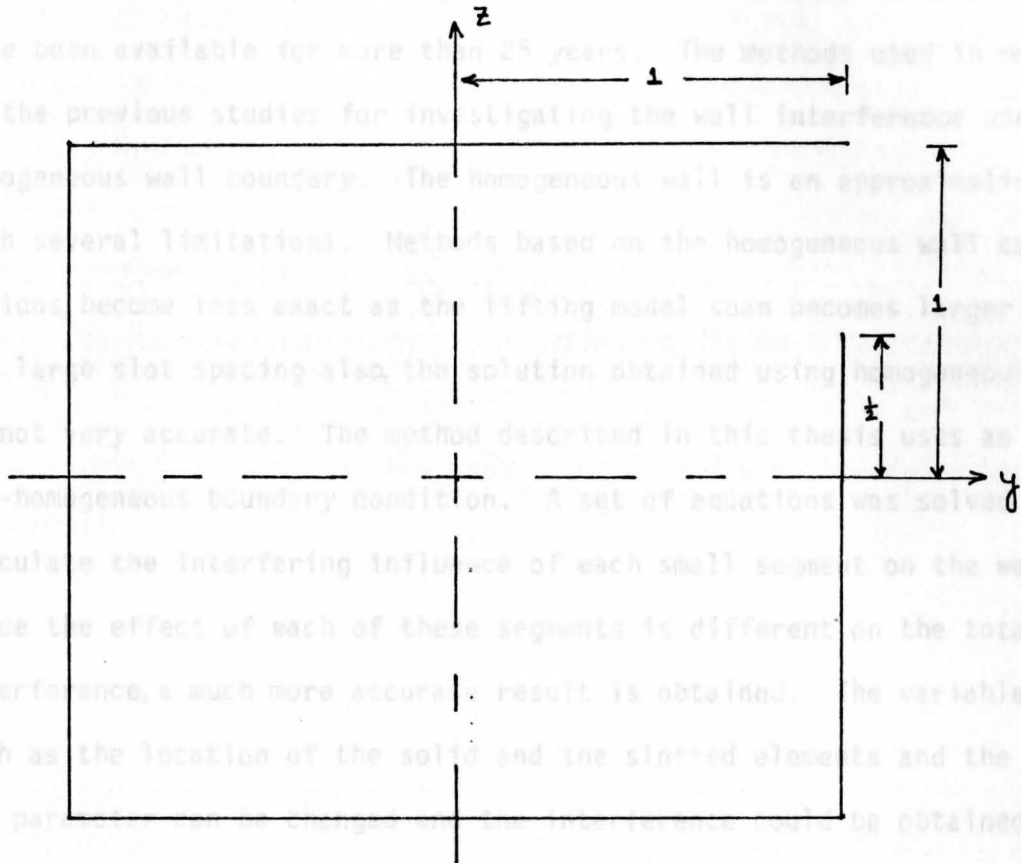


Fig. 9. Arrangement of The Wall Elements for Test Case

tunnel test, but also in designing windtunnels with minimum interference.

Conclusion

Theories for predicting the interference effects in windtunnel have been available for more than 25 years. The methods used in most of the previous studies for investigating the wall interference used a homogeneous wall boundary. The homogeneous wall is an approximation with several limitations. Methods based on the homogeneous wall conditions become less exact as the lifting model span becomes larger. For large slot spacing also, the solution obtained using homogeneous wall is not very accurate. The method described in this thesis uses an exact, non-homogeneous boundary condition. A set of equations was solved to calculate the interfering influence of each small segment on the wall. Since the effect of each of these segments is different on the total interference, a much more accurate result is obtained. The variables, such as the location of the solid and the slotted elements and the porosity parameter can be changed and the interference could be obtained by this method without any difficulty. The delta function obtained in the equations poses no problem. If the model function is divided into x - dependent and x - independent parts, the result obtained due to the delta part of the equations is the same as the result due to the x - independent part of the model potential. Hence, this method avoids the problem of splitting the problem into x - dependent and x - independent parts to obtain the total interference potential.

Recommendations

The method described in this thesis should be studied further to find its accuracy over other methods. The results obtained were only for one case in which there were very few slotted and solid elements. In such a case, the results obtained are not expected to vary much as compared to the results obtained by using homogeneous wall methods. This method is long and further study should indicate when the use of this method becomes important.

It is also recommended to investigate the wall interference obtained by changing the size and the locations of the solid and the slotted elements. A study of this kind will be useful in modifying the design of the windtunnel.

Evaluation of Equation (A-1)

Working with the equation

$$I_1 = \int_{L}^{U} K_0 \left(|q| \sqrt{(B-\xi)^2 + (y-a)^2} \right) d\xi \quad (A-3)$$

we get

$$I_1 = -\frac{1}{|q|} \int_{L}^{U} K_0 \left(\sqrt{B^2 + \xi^2} \right) d\xi \quad (A-4)$$

where,

L = lower limit

U = upper limit

$B = |q| (B-\xi)$

$\xi = |q| (y-a)$

The value of the term inside the integral in equation (A-4), is obtained by using a Bessel function relation. This relation [Ref. (2)]

APPENDIX A

The expression for the total interference potential is obtained in this appendix. To obtain this expression the following two expressions are solved first.

$$\int_{z_k}^{z_{k+1}} K_0 (|q| \sqrt{(z-\xi)^2 + (y-a)^2}) d\xi \quad (A-1)$$

$$\int_{y_k}^{y_{k+1}} K_0 (|q| \sqrt{(z-e)^2 + (y-\xi)^2}) d\xi \quad (A-2)$$

In equation (A-1), the value of a is equal to 1 for elements on the right wall and a is equal to -1 for elements on the left wall. In equation (A-2) the value of e is equal to h/b for elements on the top wall and $-h/b$ for elements on the bottom wall.

Evaluation of Equation (A-1)

Working with the equation

$$I_1 = \int_{z_k}^{z_{k+1}} K_0 (|q| \sqrt{(z-\xi)^2 + (y-a)^2}) d\xi \quad (A-3)$$

we get

$$I_1 = -\frac{1}{|q|} \int_l^u K_0 (\sqrt{\delta^2 + \varepsilon^2}) d\delta \quad (A-4)$$

where,

l = lower limit

u = upper limit

$\delta = |q| (z-\xi)$

$\varepsilon = |q| (y-a)$

The value of the term inside the integral in equation (A-4), is obtained by using a Bessel function relation. This relation [Ref. (2)]

is,

$$K_\nu(R) \cos \nu \Psi = \sum_{\lambda=-\infty}^{+\infty} K_{\nu+\lambda}(\alpha) I_\lambda(\gamma) \cos \lambda \Theta \quad (\text{A-5})$$

where

$$x - y \cos \Theta = R \cos \Psi \quad (\text{A-6})$$

$$y \sin \Theta = R \sin \Psi \quad (\text{A-7})$$

For $\Theta = \pi/2$ and $\nu = 0$ equation (A-5) can be written as,

$$K_0 \sqrt{\delta^2 + \epsilon^2} = \sum_{\lambda=-\infty}^{\infty} K_\lambda(\delta) I_\lambda(\epsilon) \cos \lambda \frac{\pi}{2} \quad (\text{A-8})$$

In the above equation x and y were replaced by δ and ϵ respectively.

Since,

$$K_\lambda(\delta) = K_{-\lambda}(\delta) \quad (\text{A-9})$$

$$I_\lambda(\epsilon) = I_{-\lambda}(\epsilon) \quad (\text{A-10})$$

equation (A-8) can be written as,

$$K_0(\sqrt{\delta^2 + \epsilon^2}) = 2 \sum_{k=1}^{\infty} (-1)^k K_{2k}(\delta) I_{2k}(\epsilon) + K_0(\delta) I_0(\epsilon) \quad (\text{A-11})$$

Substituting equation (A-11) in equation (A-4),

$$I_1 = -\frac{2}{191} \sum_{k=1}^{\infty} (-1)^k I_{2k}(\epsilon) \int_2^u K_{2k}(\delta) d\delta - \frac{I_0(\epsilon)}{9} \int_2^u K_0(\delta) d\delta \quad (\text{A-12})$$

Using power series expansion we can write,

$$K_{2k}(\delta) = \frac{1}{2} \sum_{t=0}^{2k-1} \left\{ \frac{(-1)^t (2k-t-1)!}{t!} \left(\frac{\delta}{2}\right)^{-2k+2t} + (-1)^{2k+1} \sum_{t=0}^{\infty} \left\{ \frac{(\delta/2)^{2k+2t}}{(t!)(2k+t)!} \left[\ln \frac{\delta}{2} - \frac{1}{2} \psi(t+1) - \frac{1}{2} \psi(2k+t+1) \right] \right\} \right\} \quad (\text{A-13})$$

where,

$$\psi(t+1) = \sum_{s=1}^t \frac{1}{s} - \gamma \quad (\text{A-14})$$

γ is the Euler's constant equal to 0.5772157. From mathematical tables we have,

$$K_0(|\delta|) = -\left[\gamma + \ln \frac{|\delta|}{2} \right] I_0(\delta) + \sum_{t=1}^{\infty} \left[\frac{(\delta/2)^{2t}}{(t!)^2} \sum_{s=1}^t \frac{1}{s} \right]. \quad (\text{A-15})$$

Substituting the value of $I_0(\delta)$ which is given by

$$I_0(\delta) = \sum_{t=0}^{\infty} \frac{(\delta/2)^{2t}}{(t!)^2} \quad (\text{A-16})$$

in equation (A-15) and rearranging terms we get,

$$\begin{aligned} K_0(|\delta|) &= -\sum_{t=0}^{\infty} \frac{(\delta/2)^{2t}}{(t!)^2} \ln \frac{|\delta|}{2} + \sum_{t=0}^{\infty} \frac{(\delta/2)^{2t}}{(t!)^2} (\psi(t+1) + \gamma) \\ &\quad - \frac{(\delta/2)^0}{(0!)^2} [\psi(1) + \gamma] - \sum_{t=0}^{\infty} \frac{(\delta/2)^{2t}}{(t!)^2} \gamma. \end{aligned} \quad (\text{A-17})$$

Substituting the value of $\psi(1)$ in equation (A-17) we get,

$$\begin{aligned} K_0(|\delta|) &= -\sum_{t=0}^{\infty} \frac{(\delta/2)^{2t}}{(t!)^2} \ln \frac{|\delta|}{2} + \sum_{t=0}^{\infty} \frac{(\delta/2)^{2t}}{(t!)^2} (\psi(t+1) + \gamma) \\ &\quad - \sum_{t=0}^{\infty} \frac{(\delta/2)^{2t}}{(t!)^2} \gamma. \end{aligned} \quad (\text{A-18})$$

The values of $K_{2k}(|\delta|)$ and $K_0(|\delta|)$ are substituted in equation (A-12).

Rearranging the terms,

$$\begin{aligned} I_1 &= -\frac{2}{|\delta|} \left\{ \sum_{k=1}^{\infty} (-1)^k I_{2k}(\epsilon) \left[\sum_{t=0}^{2k-1} \frac{(-1)^t (2k-t-1)!}{(t!) (-2k+2t+1)} \right] \right. \\ &\quad \left. \left(\frac{\delta}{2} \right)^{-2k+2t+1} + \sum_{t=0}^{\infty} \frac{2(\delta/2)^{2k+2t+1}}{(t!)(2k+t)!(2k+2t+1)} \right. \\ &\quad \left. \left[\frac{1}{2} \psi(t+1) + \frac{1}{2} \psi(2k+2t+1) \right] \right\} \end{aligned}$$

$$\begin{aligned}
 & - \left[\ln \frac{|\delta|}{2} + \frac{1}{2k+2t+1} \right] \\
 & + I_0(\epsilon) \sum_{t=0}^{\infty} \frac{(\delta/2)^{2t+1}}{(t!)^2 (2t+1)} \left(\psi(t+1) \right. \\
 & \left. + \frac{1}{2t+1} - \ln \frac{|\delta|}{2} \right) \Bigg\} .
 \end{aligned}$$

(A-20)

By noting that the value of $I_0(\delta)$ is,

$$I_0(\delta) = \sum_{t=0}^{\infty} \frac{(\delta/2)^{2t}}{(t!)^2}$$

(A-19)

The values of δ have an upper and lower limit in the above equation.

Putting the limits,

$$u = |\rho| (z - z_{k+1})$$

$$l = |\rho| (z - z_k)$$

in equation (A-19),

$$I_1 = - \frac{2}{|\rho|} \sum_{k=1}^{\infty} (-1)^k I_{2k}(\epsilon) \left\{ \sum_{t=0}^{2k-1} \frac{(-1)^t (2k-t-1)!}{(t!) (-2k+2t+1)} \right.$$

$$\left[\left(\frac{l}{2} \right)^{-2k+2t+1} - \left(\frac{\rho}{2} \right)^{-2k+2t+1} \right]$$

$$+ \sum_{t=0}^{\infty} \frac{2 \left[\left(\frac{l}{2} \right)^{2k+2t+1} - \left(\frac{\rho}{2} \right)^{2k+2t+1} \right]}{(t!) (2k+t)! (2k+2t+1)} \left[\frac{1}{2} \psi(t+1) + \right.$$

$$\left. \frac{1}{2} \psi(2k+2t+1) + \frac{1}{2k+2t+1} \right]$$

$$\begin{aligned}
& - \sum_{t=0}^{\infty} \frac{2 \left[\left(\frac{u}{2}\right)^{2k+2t+1} \ln \frac{1u}{2} - \left(\frac{l}{2}\right)^{2k+2t+1} \ln \frac{1l}{2} \right]}{(t!) (2t+1)! (2k+2t+1)} \Bigg\} \\
& - \frac{2}{191} I_0(\epsilon) \sum_{t=0}^{\infty} \frac{\left[\left(\frac{u}{2}\right)^{2t+1} - \left(\frac{l}{2}\right)^{2t+1} \right] \left[\psi(t+1) + \frac{1}{2t+1} \right]}{(t!)^2 (2t+1)} \\
& + \frac{2}{191} I_0(\epsilon) \sum_{t=0}^{\infty} \frac{\left[\left(\frac{u}{2}\right)^{2t+1} \ln \frac{1u}{2} - \left(\frac{l}{2}\right)^{2t+1} \ln \frac{1l}{2} \right]}{(t!)^2 (2t+1)} .
\end{aligned}$$

(A-20)

By noting that the value of $I_0(\delta)$ is,

$$I_0(\delta) = \sum_{t=0}^{\infty} \frac{(\delta/2)^{2t}}{(t!)^2} \quad (\text{A-21})$$

which can be expanded into,

$$I_0(\delta) = \frac{1}{(0!)^2} + \frac{(\delta/2)^2}{(1!)^2} + \frac{(\delta/2)^4}{(2!)^2} + \dots \quad (\text{A-22})$$

we obtain $I_0(0) = 1$ for $\delta = 0$. Similarly the value of $I_{2k}(0)$ can be obtained as zero. The values of $I_0(0)$ and $I_{2k}(0)$ can be substituted in equation (A-20) to obtain the value of I_1 .

From equation (A-20), we can see that I_1 is a function of ϵ , u and l . Hence we can write,

$$I_1 = G_1(\epsilon, u, l) . \quad (\text{A-23})$$

Since the values of ϵ , u and l are different for each element, the value of I_1 depends upon the location of the element. The expressions for I_1 for different locations of the elements are shown below.

Element On the Right Wall

The value of δ tends to $|\rho|(\bar{z}_n - z)$ as z tends to \bar{z}_n . If z_k and z_{k+1} are the lower and the upper limits of the element located on the right wall and \bar{z}_n is outside the interval z_k to z_{k+1} then,

$$I_1 = G_1(0, |\rho|(\bar{z}_n - z_{k+1}), |\rho|(\bar{z}_n - z_k)) \quad (A-24)$$

In the above equation y tends to a , hence ϵ tends to zero.

Element on the Left Wall

For a wall element on the left wall, z tends to \bar{z}_n and y tends to $-a$. Hence,

$$\epsilon = -2a|\rho|$$

$$u = |\rho|(\bar{z}_n - z_{k+1})$$

$$l = |\rho|(\bar{z}_n - z_k)$$

Therefore,

$$I_1 = G_1(-2a|\rho|, |\rho|(\bar{z}_n - z_{k+1}), |\rho|(\bar{z}_n - z_k)) \quad (A-25)$$

Element on the Upper Wall

For the wall element on the upper wall, z tends to h/b and y tends to \bar{y}_n . Therefore,

$$\epsilon = |\rho|(\bar{y}_n - a)$$

$$u = |\rho|(h/b - z_{k+1})$$

$$l = |\rho|(h/b - z_k)$$

Using the above expressions for ϵ , u and l we can write equation (A-23)

as,

$$I_1 = G_1(|\rho|(\bar{y}_n - a), |\rho|(h/b - z_{k+1}), |\rho|(h/b - z_k)) \quad (A-26)$$

Element On the Lower Wall

For an element on the lower wall z tends to $-h/b$ and y tends to \bar{y}_n . The value of I_1 for these elements is given by,

$$I_1 = G_1 \left(|\rho| (\bar{y}_n - a), |\rho| \left(-\frac{h}{b} - z_{k+1}\right), |\rho| \left(-\frac{h}{b} - z_k\right) \right) \quad (A-27)$$

Expression for I_1 when \bar{z}_n is midway between z_k and z_{k+1}

If \bar{z}_n is midway between z_k and z_{k+1} , then z is equal to $\frac{u+1}{2}$.

The expression for I_1 is given by,

$$I_1 = - \int_{|\rho|(z-\epsilon)}^{|\rho|(z-u)} \frac{K_0 \sqrt{\delta^2 + \epsilon^2}}{|\rho|} d\delta \quad (A-28)$$

Substituting the value of z we get,

$$I_1 = \int_{|\rho|\frac{(u-\epsilon)}{2}}^{|\rho|\frac{(u-u)}{2}} \frac{-K_0 \sqrt{\delta^2 + \epsilon^2}}{|\rho|} d\delta \quad (A-29)$$

If we write $(u-1)$ equal to Δz , then equation (A-29) can be written

$$I_1 = \int_{|\rho|\frac{\Delta z}{2}}^{|\rho|\frac{\Delta z}{2}} \frac{K_0 \sqrt{\delta^2 + \epsilon^2}}{|\rho|} d\delta \quad (A-30)$$

By changing the limits and reversing the sign of the upper limit we can write the above equation as,

$$I_1 = 2 \int_0^{|\rho|\frac{\Delta z}{2}} \frac{K_0 \sqrt{\delta^2 + \epsilon^2}}{|\rho|} d\delta \quad (A-31)$$

For a wall element at y equal to a , the value of ϵ is equal to zero.

Now, putting the limits

$$u = |\rho| \frac{\Delta z}{2}$$

$$\ell = 0$$

$$\epsilon = 0$$

in equation (A-23), we get

$$I_1 = -2 G_1 \left(0, |\rho| \frac{\Delta z}{2}, 0 \right) \quad (A-32)$$

Evaluation of Equation (A-2)

The solution of equation (A-2) is analogous to the solution of equation (A-1). The expression for I_2 is given by,

$$\int_{y_k}^{y_{k+1}} K_0 (191 \sqrt{(z-e)^2 + (y-\xi)^2}) d\xi = I_2 \quad (A-33)$$

The value of I_2 can be obtained for any wall element by replacing z with y , a with e and y with z . The solutions obtained after these replacements are given below.

When \bar{y}_n is midway between the interval y_k to y_{k+1} the solution is analogous to equation (A-32). It is given by,

$$I_2 = -2G_1 \left(0, \frac{191}{2} (y_{k+1} - y_k), 0 \right) \quad (A-34)$$

If \bar{y}_n is outside the interval y_k to y_{k+1} , then the value of I_2 depends upon the location of the element. For an element located on the upper wall, the expression is given by,

$$I_2 = G_1 \left(0, 191 (\bar{y}_n - y_{k+1}), 191 (\bar{y}_n - y_k) \right) \quad (A-35)$$

If the element is located on the bottom wall the value of I_2 is given by,

$$I_2 = G_1 \left(-2e191, 191 (\bar{y}_n - y_{k+1}), 191 (\bar{y}_n - y_k) \right) \quad (A-36)$$

If the element is on the right wall, y tends to 1 and the expression for I_2 is given by,

$$I_2 = G_1 \left(191 (\bar{z}_n - e), 191 (1 - y_{k+1}), 191 (1 - y_k) \right) \quad (A-37)$$

For the element on the left wall y tends to -1 and I_2 is obtained from the expression,

$$I_2 = G_1 \left(191 (\bar{z}_n - e), 191 (-1 - y_{k+1}), 191 (-1 - y_k) \right) \quad (A-38)$$

Total Interference Potential

The general expression for the interference potential expressed as the sum of the contributions from each element is given by,

$$\phi_i = \sum_{\text{ENTIRE BODY}} \int \sigma_k \kappa_0 (r') d\zeta \quad (\text{A-39})$$

In the above equation r' is the distance from each element to the point in space where the value of ϕ_i is desired. The equation is summed over the entire body because the total interference due to any element, is the sum of the interference of each element evaluated at this element. The total interference potential of an element, for the two different cases, is given below.

Element Located At $y = 1, 0 < z < h/b$

Figure 10 shows the location of this element.

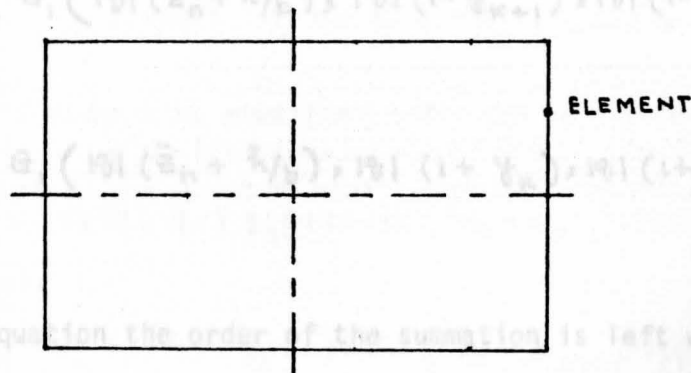


Figure 10. Element located at $y = 1$ and $0 < z < h/b$

For this element n , equation (A-39) can be expanded into,

$$\phi_i = \sum_{k=1}^{K_i} \sigma_k G_i (2|r'|, |r'| (\bar{z}_n - z_{k+1}), |r'| (\bar{z}_n - z_k))$$

$$\begin{aligned}
& - \sum_{k=1}^{K_1} \sigma_k G_1(2\rho_1, \rho_1(\bar{z}_n + z_{k+1}), \rho_1(\bar{z}_n + z_k)) \\
& + \sum_{k=1}^{K_1} \sigma_k G_1(0, \rho_1(\bar{z}_n - z_{k+1}), \rho_1(\bar{z}_n - z_k)) \\
& + \sum_{k=1}^{n-1} \sigma_k G_1(0, \rho_1(\bar{z}_n - z_{k+1}), \rho_1(\bar{z}_n - z_k)) \\
& - 2 \sigma_n G_1(0, \frac{\rho_1}{2}(z_{k+1} - z_k), 0) \\
& - \sum_{k=1}^{K_1} \sigma_k G_1(0, \rho_1(\bar{z}_n + z_{k+1}), \rho_1(\bar{z}_n + z_k)) \\
& + \sum_{k=K_1+1}^{K_2} \sigma_k G_1(\rho_1(\bar{z}_n - h/b), \rho_1(1 - \gamma_{k+1}), \rho_1(1 - \gamma_k)) \\
& + \sum_{k=K_1+1}^{K_2} \sigma_k G_1(\rho_1(\bar{z}_n - h/b), \rho_1(1 + \gamma_k), \rho_1(1 + \gamma_{k+1})) \\
& - \sum_{k=K_1+1}^{K_2} \sigma_k G_1(\rho_1(\bar{z}_n + h/b), \rho_1(1 - \gamma_{k+1}), \rho_1(1 - \gamma_k)) \\
& - \sum_{k=K_1+1}^{K_2} \sigma_k G_1(\rho_1(\bar{z}_n + h/b), \rho_1(1 + \gamma_k), \rho_1(1 + \gamma_{k+1})) .
\end{aligned} \tag{A-40}$$

In the above equation the order of the summation is left wall top half, left wall bottom half, right wall top half, element n, right wall bottom half, top wall right half, top wall left half, bottom wall right half and bottom wall left half. To simplify equation (A-40) we can write the total interference potential due to element n as,

$$\phi_i = W_3(n, q) . \tag{A-41}$$

The function $W_3(n, q)$ has a real and an imaginary part since the influence coefficient, σ_k , in equation (A-40) is a complex function. Let prime and double prime represent the real and imaginary part of the interference potential. Then, the real part is,

$$W_3' (n, q) = \left[W_3(n, q) \right]_{\text{At } \sigma_k = \sigma_k'} \quad (\text{A-42})$$

and the imaginary part is,

$$W_3'' (n, q) = \left[W_3(n, q) \right]_{\text{At } \sigma_k = \sigma_k''} \quad (\text{A-43})$$

In the above equations σ_k' and σ_k'' are the real and the imaginary parts of the influence coefficient.

Element Located At $z = h/b, 0 < y < 1$

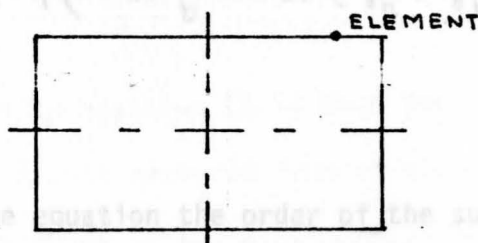


Figure 11. Element located at $z = h/b, 0 < y < 1$

For this element n , equation (A-39) can be expanded into,

$$\begin{aligned} \Phi_i = & \sum_{k=1}^{K_1} \sigma_k G_1 \left(|q| (\bar{y}_n + 1), |q| (h/b - z_{k+1}), |q| (h/b - z_k) \right) \\ & - \sum_{k=1}^{K_1} \sigma_k G_1 \left(|q| (\bar{y}_n + 1), |q| (h/b + z_{k+1}), |q| (h/b + z_k) \right) \\ & + \sum_{k=1}^{K_1} \sigma_k G_1 \left(|q| (\bar{y}_n - 1), |q| (h/b - z_{k+1}), |q| (h/b - z_k) \right) \\ & - \sum_{k=1}^{K_1} \sigma_k G_1 \left(|q| (\bar{y}_n - 1), |q| (h/b + z_{k+1}), |q| (h/b + z_k) \right) \\ & + \sum_{k=n+1}^{K_2} \sigma_k G_1 \left(0, |q| (\bar{y}_n - y_{k+1}), |q| (\bar{y}_n - y_k) \right) \end{aligned}$$

$$\begin{aligned}
& + \sum_{K=K_1+1}^{n-1} \sigma_K G_1(0, 191(\bar{y}_n - y_{K+1}), 191(\bar{y}_n - y_K)) \\
& - 2 \sigma_n G_1\left(0, \frac{191}{2}(y_{K+1} - y_K), 0\right) \\
& + \sum_{K=K_1+1}^{K_2} \sigma_K G_1\left(0, 191(\bar{y}_n + y_{K+1}), 191(\bar{y}_n + y_K)\right) \\
& - \sum_{K=K_1+1}^{K_2} \sigma_K G_1\left(2 \cdot 191 \frac{h}{b}, 191(\bar{y}_n - y_{K+1}), 191(\bar{y}_n - y_K)\right) \\
& - \sum_{K=K_1+1}^{K_2} \sigma_K G_1\left(2 \cdot 191 \frac{h}{b}, 191(\bar{y}_n + y_{K+1}), 191(\bar{y}_n + y_K)\right).
\end{aligned}$$

(A-44)

In the above equation the order of the summation is left wall top half, left wall bottom half, right wall top half, right wall bottom half, top wall right half, element n, top wall left half, bottom wall right half, and bottom wall left half. The right hand side of equation (A-44) can be given by,

$$\phi_i = W_4(n, q). \quad (A-45)$$

For a complex influence coefficient the real and the imaginary parts of $W_4(n, q)$ are,

$$W_4'(n, q) = \boxed{W_4(n, q)}_{\sigma_K = \sigma_K'} \quad (A-46)$$

$$W_4''(n, q) = \boxed{W_4(n, q)}_{\sigma_K = \sigma_K''} \quad (A-47)$$

Substituting,

APPENDIX B

For any wall element on the boundary, the expression

$$\frac{\partial}{\partial n} \int K_0 (|r| r') d\xi \quad (B-1)$$

is evaluated in this appendix. In the above equation n is the normal coordinate y or z . Then, the above integral is expressed for the entire boundary, evaluated at any n^{th} wall element on $z = h/b$, $y \leq 1$ (top wall, right half) and for any n^{th} wall element on $y = 1$, $z \leq h/b$ (right wall, top half).

General Expression for I_3

I_3 is given by equation (B-1) when the normal coordinate is y and the distance, r' , is measured from an element on the right or the left wall to any point in the windtunnel. The expression for I_3 is,

$$\frac{\partial}{\partial y} \int_{z_k}^{z_{k+1}} K_0 (|r| \sqrt{(z-\xi)^2 + (y-a)^2}) d\xi = I_3 \quad (B-2)$$

where, $a = 1$ for elements on the right wall and $a = -1$ for elements on the left wall.

Equation (B-2) can be written as,

$$I_3 = \int_{z_k}^{z_{k+1}} \frac{\partial K_0 (|r| \sqrt{(z-\xi)^2 + (y-a)^2})}{\partial (|r| \sqrt{(z-\xi)^2 + (y-a)^2})} \left[\frac{|r| (y-a)}{\sqrt{(z-\xi)^2 + (y-a)^2}} \right] d\xi \quad (B-3)$$

Differentiating equation (B-3),

$$I_3 = \int_{z_k}^{z_{k+1}} \frac{-K_1 (|r| \sqrt{(z-\xi)^2 + (y-a)^2})}{\sqrt{(z-\xi)^2 + (y-a)^2}} \left[|r| (y-a) \right] d\xi \quad (B-4)$$

Substituting,

$$\delta = |\rho| (z - \zeta)$$

$$\epsilon = |\rho| (y - a)$$

$$d\delta = -|\rho| d\zeta$$

(B-5)

in equation (B-4)

$$I_3 = \int_l^u \frac{\epsilon}{\delta} \left[\frac{-\delta K_1(\sqrt{\delta^2 + \epsilon^2})}{\sqrt{\delta^2 + \epsilon^2}} \right] d\delta \quad (B-6)$$

where,

$$u = |\rho| (z - z_{k+1})$$

$$l = |\rho| (z - z_k)$$

Noting that,

$$\frac{d}{d\delta} \left[K_0 \sqrt{\delta^2 + \epsilon^2} \right] = \frac{-\delta K_1(\sqrt{\delta^2 + \epsilon^2})}{\sqrt{\delta^2 + \epsilon^2}} \quad (B-7)$$

and integrating equation (B-6) by parts,

$$I_3 = -\frac{\epsilon}{\delta} K_0(\sqrt{\delta^2 + \epsilon^2}) \Big|_l^u - \epsilon \int_l^u \frac{K_0(\sqrt{\delta^2 + \epsilon^2})}{\delta^2} d\delta \quad (B-8)$$

Substituting the value of $K_0 \sqrt{\delta^2 + \epsilon^2}$ from equation (A-33) in appendix (A), in equation (B-7), and evaluating the integral,

$$-\epsilon \int \frac{K_0(\sqrt{\delta^2 + \epsilon^2})}{\delta^2} d\delta = -2\epsilon \sum_{t=1}^{\infty} (-1)^t K_{2t}(|\epsilon|) \int \frac{I_{2t}(\delta)}{\delta^2} d\delta$$

$$= -\epsilon K_0(|\epsilon|) \int \frac{I_0(\delta)}{\delta^2} d\delta \quad (B-9)$$

Substituting,

$$I_{2t}(\delta) = \sum_{k=0}^{\infty} \frac{(\frac{\delta}{2})^{2t+2k}}{k! (2t+k)!} \quad (B-10)$$

$$I_0(\delta) = \sum_{k=0}^{\infty} \frac{(\frac{\delta}{2})^{2k}}{(k!)^2} \quad (B-11)$$

in equation (B-9) and integrating the right hand side,

$$\begin{aligned} -\epsilon \int \frac{K_0(\sqrt{\delta^2 + \epsilon^2})}{\delta^2} d\delta &= -\epsilon \sum_{t=1}^{\infty} (-1)^t K_{2t}(|\epsilon|) \sum_{k=0}^{\infty} \frac{(\frac{\delta}{2})^{2t+2k-1}}{k! (2t+k)! (2t+2k-1)} \\ &\quad - \frac{\epsilon}{2} K_0(|\epsilon|) \sum_{k=0}^{\infty} \frac{(\frac{\delta}{2})^{2k-1}}{(k!) (2k-1)}. \end{aligned} \quad (B-12)$$

Inserting equation (B-12) into equation (B-8) and putting the upper and the lower limit in the equation,

$$\begin{aligned} I_3 &= -\frac{\epsilon}{u} K_0(\sqrt{u^2 + \epsilon^2}) + \frac{\epsilon}{l} K_0(\sqrt{l^2 + \epsilon^2}) \\ &\quad - \epsilon \sum_{t=1}^{\infty} (-1)^t K_{2t}(|\epsilon|) \sum_{k=0}^{\infty} \frac{(\frac{u}{2})^{2t+2k-1} - (\frac{l}{2})^{2t+2k-1}}{(k!) (2t+k)! (2t+2k-1)} \\ &\quad - \frac{\epsilon}{2} K_0(|\epsilon|) \sum_{k=0}^{\infty} \frac{(\frac{u}{2})^{2k-1} - (\frac{l}{2})^{2k-1}}{(k!)^2 (2k-1)}. \end{aligned} \quad (B-13)$$

From equation (B-13), I_3 can be shown to be a function ϵ , u and l . Hence,

$$I_3 = F_1(\epsilon, u, l) \quad (B-14)$$

where, the function F_1 is defined by equation (B-13) and the values of ϵ , u and l are given by,

$$\begin{aligned} \epsilon &= |y| (y-a) \\ u &= |y| (z - z_{k+1}) \\ l &= |y| (z - z_k) \end{aligned} \quad (B-15)$$

Equations (B-13) and (B-14) give the general expression for I_3 .

Evaluation of I_3 for $y = a$ and $z = \bar{z}_n$

\bar{z}_n Midway Between Z_k and Z_{k+1} on $y = a$

The value of I_3 for an element at $y = a$ can be obtained by substituting equation (B-5) in equation (B-4), if \bar{z}_n lies between the limits Z_k and Z_{k+1} of the element. When $Z_k < \bar{z}_n < Z_{k+1}$, we assume that \bar{z}_n lies in the middle of the element. The equation for I_3 is,

$$I_3 = \int_l^u \frac{\epsilon K_1(\sqrt{\delta^2 + \epsilon^2})}{\sqrt{\delta^2 + \epsilon^2}} d\delta. \quad (B-16)$$

The limits u and l are defined by equation (B-15). The term $K_1(\sqrt{\delta^2 + \epsilon^2})$ in equation (B-16) can be expanded into [Ref. (2)],

$$K_1(\sqrt{\delta^2 + \epsilon^2}) = \left\{ \gamma + \ln \frac{\sqrt{\delta^2 + \epsilon^2}}{2} \right\} \sum_{\lambda=0}^{\infty} \frac{1}{(\lambda!)(\lambda+1)!} \left[\frac{\sqrt{\delta^2 + \epsilon^2}}{2} \right]^{2\lambda+1} \\ + \frac{1}{\sqrt{\delta^2 + \epsilon^2}} - \sum_{\lambda=0}^{\infty} \frac{1}{(\lambda!)(\lambda+1)!} \left[\frac{\sqrt{\delta^2 + \epsilon^2}}{2} \right]^{2\lambda+1} \left[\sum_{s=1}^{\lambda} \frac{1}{s} + \frac{1}{2(\lambda+1)} \right]. \quad (B-17)$$

Rearranging equation (B-17),

$$K_1(\sqrt{\delta^2 + \epsilon^2}) = \left\{ \gamma + \ln \frac{\sqrt{\delta^2 + \epsilon^2}}{2} \right\} \left\{ \frac{\sqrt{\delta^2 + \epsilon^2}}{4} + \frac{1}{2} \left(\frac{\sqrt{\delta^2 + \epsilon^2}}{4} \right)^3 \right. \\ \left. + \text{higher odd powers of } \sqrt{\delta^2 + \epsilon^2} \right\} + \left\{ \frac{1}{\sqrt{\delta^2 + \epsilon^2}} - \frac{\sqrt{\delta^2 + \epsilon^2}}{4} \right. \\ \left. + \text{higher odd powers of } \sqrt{\delta^2 + \epsilon^2} \right\}. \quad (B-18)$$

Substituting equation (B-18) in equation (B-16),

$$I_3 = \int_l^u \frac{\epsilon}{\delta^2 + \epsilon^2} d\delta. \quad (B-19)$$

All the other terms of equation (B-18) can be neglected as ϵ tends to zero. Integrating equation (B-19),

The value of a is equal to 1 for the right wall. Hence the value of ϵ tends to 0^+ as y tends to a . Putting these limits in equation (B-20)

$$I_3 = \left[\tan^{-1} \frac{\delta}{\epsilon} \right]_l^u. \quad (B-20)$$

The above equation gives the value of I_3 for an element on the side walls. The value of I_3 for the left and the right wall are shown below.

I_3 For the Left Wall

For the left wall a is equal to -1 . In this case when y tends to $-a$, the value of ϵ which is given by equation (B-5) tends to 0^+ . Putting these limits in equation (B-20),

$$I_3 = \tan^{-1} \left[\frac{191(\bar{z}_n - z_{k+1})}{0^+} \right] - \tan^{-1} \left[\frac{191(\bar{z}_n - z_k)}{0^+} \right]. \quad (B-21)$$

Evaluating the right hand side of equation (B-21),

The value of I_3 for $y = a$ and $z = \bar{z}_n$, where \bar{z}_n is midway between z_k and z_{k+1}

$$I_3 = \pi \quad (B-22)$$

when, $z_k < \bar{z}_n < z_{k+1}$. From equation (B-15) the value of ϵ for the element at $y = -a$ is,

If \bar{z}_n is not between z_k and z_{k+1} ,

$$\epsilon = -2a191. \quad (B-27)$$

$$I_3 = 0. \quad (B-23)$$

Using equation (B-27) and equation (B-14), the value of I_3 is,

$$I_3 = F_1 [-2a191, 191(\bar{z}_n - z_{k+1}), 191(\bar{z}_n - z_k)]. \quad (B-28)$$

I_3 For the Right Wall General Expression For I_3

The value of a is equal to 1 for the right wall. Hence the value of ϵ tends to 0^- as y tends to a . Putting these limits in equation (B-20),

$$I_3 = \tan^{-1} \left[\frac{191(\bar{z}_n - z_{k+1})}{0^-} \right] - \tan^{-1} \left[\frac{191(\bar{z}_n - z_k)}{0^-} \right] \quad (B-24)$$

Evaluating the right hand side of equation (B-24),

$$I_3 = \pi \quad (B-25)$$

when, $z_k < \bar{z}_n < z_{k+1}$

If \bar{z}_n is not between z_k and z_{k+1} ,

$$I_3 = 0 \quad (B-26)$$

\bar{z}_n Midway Between z_k and z_{k+1} on $y = -a$

The value of I_3 for $y = a$ and $z = \bar{z}_n$, where \bar{z}_n is midway between z_k and z_{k+1} at the n^{th} wall element on $y = -a$, can be obtained from equation (B-14). From equation (B-15) the value of ϵ for the element at $y = -a$ is,

$$\epsilon = -2a191 \quad (B-27)$$

Using equation (B-27) and equation (B-14), the value of I_3 is,

$$I_3 = F_1 \left[-2a191, 191(\bar{z}_n - z_{k+1}), 191(\bar{z}_n - z_k) \right] \quad (B-28)$$

General Expression For I_4

Equation (B-1) is denoted by I_4 when the normal coordinate is z and r' is the distance between the side walls and any point in the tunnel. Therefore,

$$\frac{\partial}{\partial z} \int_{z_k}^{z_{k+1}} K_0 (191 \sqrt{(z-\xi)^2 + (y-a)^2}) d\xi = I_4. \quad (\text{B-29})$$

Differentiating equation (B-29),

$$\int_{z_k}^{z_{k+1}} \frac{K_1 (191 \sqrt{(z-\xi)^2 + (y-a)^2})}{\sqrt{(z-\xi)^2 + (y-a)^2}} d\xi. \quad (\text{B-30})$$

Substituting

$$\delta = 191(z - \xi)$$

$$\epsilon = 191(y - a)$$

$$d\delta = -191 d\xi \quad (\text{B-31})$$

in equation (B-30) the value of I_4 can be written as,

$$I_4 = - \int_{\ell}^u \frac{-K_1 (\sqrt{\delta^2 + \epsilon^2})}{\sqrt{\delta^2 + \epsilon^2}} \delta d\delta. \quad (\text{B-32})$$

Using ref (2), we note that,

$$\frac{d}{d\delta} \left[K_0 (\sqrt{\delta^2 + \epsilon^2}) \right] = \frac{-\delta K_1 (\sqrt{\delta^2 + \epsilon^2})}{\sqrt{\delta^2 + \epsilon^2}}. \quad (\text{B-33})$$

Hence the integral of equation (B-32) is given by,

$$I_4 = - \left[K_0 (\sqrt{\delta^2 + \epsilon^2}) \right]_{\ell}^u \quad (B-34)$$

Putting the limits in equation (B-34),

$$I_4 = - K_0 (\sqrt{u^2 + \epsilon^2}) + K_0 (\sqrt{\ell^2 + \epsilon^2}) \quad (B-35)$$

From equation (B-35) I_4 is a function of ϵ , u and ℓ . Therefore we can express I_4 as a function of these three variables. That is,

$$I_4 = F_2(\epsilon, u, \ell) \quad (B-36)$$

The function F_2 is defined by equation (B-35) and the arguments ϵ , u and ℓ are,

$$\begin{aligned} \epsilon &= |y - a| \\ u &= |z - z_{k+1}| \\ \ell &= |z - z_k| \end{aligned} \quad (B-37)$$

Evaluation of I_4 For $z = e$ and $y = \bar{y}_n$

For $z = e$ and $y = \bar{y}_n$, the value of I_4 can be obtained by using equation (B-36) and (B-37). The expression e is h/b for the top wall and e is $-h/b$ for the bottom wall. If \bar{y}_n is the center of the n^{th} wall element on $z = e$, then I_4 is given by,

$$I_4 = F_2 \left[|y_n - a|, |e - z_{k+1}|, |e - z_k| \right] \quad (B-38)$$

General Expression For I_5

If the normal coordinate is z and r' is the distance from the

top or the bottom wall to any point in the windtunnel, then equation (B-1) is denoted by I_5 . Therefore,

$$I_5 = \frac{\partial}{\partial z} \int_{y_k}^{y_{k+1}} K_0 (191 \sqrt{(z-e)^2 + (y-\xi)^2}) d\xi. \quad (B-39)$$

Comparing equation (B-39) with equation (B-2), we see that if y and z are interchanged and if e and a are interchanged, the result given by equation (B-13) can be used. Therefore,

$$I_5 = F_1 \left[191(z-e), 191(y-y_{k+1}), 191(y-y_k) \right]. \quad (B-40)$$

Evaluation of I_5 For $z = e$ And $y = \bar{y}_n$

\bar{y}_n At The Center of n^{th} Wall Element On The Wall $z = e$

Using the result in equation (B-22) and equation (B-25) the value of I_5 for $z = e$ and $y = \bar{y}_n$ is,

$$I_5 = \pi \quad (B-41)$$

when $y_k < \bar{y}_n < y_{k+1}$. Here, y_k and y_{k+1} are the limits of the element for which the value of I_5 is being calculated. If \bar{y}_n does not lie between y_k and y_{k+1} , then from equation (B-23) and equation (B-26) the value of I_5 is given by,

$$I_5 = 0. \quad (B-42)$$

\bar{y}_n At The Center of n^{th} Wall Element On The Wall $z = -e$

The value of I_5 for $z = e$ and $y = \bar{y}_n$ can be obtained by using the result given by equation (B-28). Here, \bar{y}_n is the center of the n^{th} wall element on the wall $z = -e$. Replacing z and a in equation (B-28) with y and e respectively, we get,

$$I_5 = F_1 \left[-2e|a_1|, |a_1|(\bar{y}_n - y_{k+1}), |a_1|(\bar{y}_n - y_k) \right] \quad (B-43)$$

General Expression For I_6

If the normal coordinate is y and the distance, r' , is measured from the top or the bottom wall, then equation (B-1) is denoted by I_6 .

Therefore,

$$I_6 = \frac{\partial}{\partial y} \int_{y_k}^{y_{k+1}} K_0 (|a_1| \sqrt{(z-e)^2 + (y-\xi)^2}) d\xi \quad (B-44)$$

Comparing equation (B-44) with equation (B-29), we see that if y and z are interchanged and e and a are interchanged, the result given by equation (B-36) can be used as the solution of equation (B-44). That is,

$$I_6 = F_2 \left[|a_1|(z-e), |a_1|(y-y_{k+1}), |a_1|(y-y_k) \right] \quad (B-45)$$

Evaluation of I_6 For $y = a$ and $z = \bar{z}_n$

\bar{z}_n At The Center of n^{th} Wall Element On The Wall $y = a$

The value of I_6 for $y = a$ and $z = \bar{z}_n$, where \bar{z}_n is the center of the n^{th} element on the wall $y = a$, is obtained by putting the limits in equation (B-45). Therefore,

$$\lim_{\substack{y \rightarrow a \\ z \rightarrow \bar{z}_n}} I_6 = F_2 \left[|a_1|(\bar{z}_n - e), |a_1|(a - y_{k+1}), |a_1|(a - y_k) \right] \quad (B-46)$$

Expression For the Entire Boundary

Equation (B-1) multiplied by the influence coefficient of the elements is,

$$\frac{\partial}{\partial \pi} \int \sigma_k k_0 (|\rho| \rho') d\xi \quad (B-47)$$

Equation (B-47) is expressed below for the entire wall boundary. The expression depends upon the location of the element.

Wall Element At $y = 1, 0 < z < h/b$

Expressing equation (B-47) for the entire boundary, evaluated at the n^{th} element on the wall $y = 1, 0 < z < h/b$,

$$\sum_{\text{Entire Boundary}} \sigma_k \frac{\partial}{\partial y} \int k_0 (|\rho| \rho') d\xi. \quad (B-48)$$

Expanding equation (B-48),

$$\begin{aligned} & \sum_{k=1}^{K_1} \sigma_k F_1 \left[2|\rho|, |\rho| (\bar{z}_n - z_{k+1}), |\rho| (\bar{z}_n - z_k) \right] \\ & - \sum_{k=1}^{K_1} \sigma_k F_1 \left[2|\rho|, |\rho| (\bar{z}_n + z_k), |\rho| (\bar{z}_n + z_{k+1}) \right] \\ & + \sigma_n (\pi) \\ & + \sum_{k=K_1+1}^{K_2} \sigma_k F_2 \left[|\rho| (\bar{z}_n - \frac{h}{b}), |\rho| (1 - \gamma_{k+1}), |\rho| (1 - \gamma_k) \right] \\ & + \sum_{k=K_1+1}^{K_2} \sigma_k F_2 \left[|\rho| (\bar{z}_n - \frac{h}{b}), |\rho| (1 + \gamma_k), |\rho| (1 + \gamma_{k+1}) \right] \\ & - \sum_{k=K_1+1}^{K_2} \sigma_k F_2 \left[|\rho| (\bar{z}_n + \frac{h}{b}), |\rho| (1 - \gamma_{k+1}), |\rho| (1 - \gamma_k) \right] \end{aligned}$$

Expanding equation (B-53).

$$- \sum_{k=k_1+1}^{k_2} \sigma_k F_2 \left[|q| (\bar{z}_n + h/b), |q| (1 + y_k), |q| (1 + y_{k+1}) \right]. \quad (B-49)$$

The terms in the above equation are due to the left wall top half, left wall bottom half, right wall, top wall right half, top wall left half, bottom wall right half and the bottom wall left half. Equation (B-49) is a function of q and the location of the element, n . Therefore the above equation can be expressed as,

$$\sum_{\text{Entire Boundary}} \sigma_k \frac{\partial}{\partial y} \int k_0 (|q| z') d\xi = W_1(n, q). \quad (B-50)$$

For a complex influence coefficient we get a real and an imaginary value of $W_1(n, q)$. The real value is,

$$W_1'(n, q) = \left[W_1(n, q) \right]_{\sigma_k = \sigma_k'} \quad (B-51)$$

and the imaginary value is,

$$W_1''(n, q) = \left[W_1(n, q) \right]_{\sigma_k = \sigma_k''}. \quad (B-52)$$

The primes and the double primes indicate the real and the imaginary values respectively.

Wall Element At $z = h/b, 0 < y < 1$

Expressing equation (B-47) for the entire boundary, evaluated at the n^{th} element on the wall $z = h/b, 0 < y < 1$,

$$\sum_{\text{Entire Boundary}} \sigma_k \frac{\partial}{\partial z} \int k_0 (|q| z') d\xi. \quad (B-53)$$

Expanding equation (B-53),

$$\begin{aligned}
 & \sum_{k=1}^{K_1} \sigma_k F_2 \left[\rho_1 (\bar{y}_n + 1), \rho_1 (h/b - z_{k+1}), \rho_1 (h/b - z_k) \right] \\
 & - \sum_{k=1}^{K_1} \sigma_k F_2 \left[\rho_1 (\bar{y}_n + 1), \rho_1 (h/b + z_{k+1}), \rho_1 (h/b + z_k) \right] \\
 & + \sigma_n (\pi) \\
 & + \sum_{k=1}^{K_1} \sigma_k F_2 \left[\rho_1 (\bar{y}_n - 1), \rho_1 (h/b - z_{k+1}), \rho_1 (h/b - z_k) \right] \\
 & - \sum_{k=1}^{K_1} \sigma_k F_2 \left[\rho_1 (\bar{y}_n - 1), \rho_1 (h/b + z_{k+1}), \rho_1 (h/b + z_k) \right] \\
 & - \sum_{k=K_1+1}^{K_2} \sigma_k F_1 \left[2\rho_1 \frac{h}{b}, \rho_1 (\bar{y}_n - y_{k+1}), \rho_1 (\bar{y}_n - y_k) \right] \\
 & - \sum_{k=K_1+1}^{K_2} \sigma_k F_1 \left[2\rho_1 \frac{h}{b}, \rho_1 (\bar{y}_n + y_{k+1}), \rho_1 (\bar{y}_n + y_k) \right].
 \end{aligned}$$

(B-54)

The terms in the above equation are due to the left wall top half, left wall bottom half, top wall, right wall top half, right wall bottom half, bottom wall right half and the bottom wall left half. Equation (B-54) is a function of q and the location of the element, n . Therefore, the above equation is expressed as,

$$\sum \sigma_k \frac{\partial}{\partial z} \int K_0(|\rho|, \rho') d\xi = W_2(n, q).$$

Entire Boundary (B-55)

For a complex influence coefficient we get a real and an imaginary value of $W_2(n, q)$. The real value is,

$$W_2' (n, q) = [W_2(n, q)]_{\sigma_k = \sigma_k'} \quad (B-56)$$

$$W_2'' (n, q) = [W_2(n, q)]_{\sigma_k = \sigma_k''} \quad (B-57)$$

The primes and the double primes indicate the real and the imaginary values respectively.

$$\begin{aligned} (\bar{\Phi}_m)_j &= \frac{\Gamma_1 \Delta y_j}{4\pi} \left[1 + \frac{(x-x_j)}{\sqrt{(x-x_j)^2 + \rho^2 [(y-y_j)^2 + z^2]}} \right] \left[\frac{z}{(y-y_j)^2 + z^2} \right] \\ &+ \frac{\Gamma_2 \Delta y_j}{4\pi} \left[1 + \frac{(x-x_j)}{\sqrt{(x-x_j)^2 + \rho^2 [(y+y_j)^2 + z^2]}} \right] \left[\frac{z}{(y+y_j)^2 + z^2} \right]. \quad (C-2) \end{aligned}$$

In normalized form this model potential can be written as,

$$\begin{aligned} (\Phi_m)_j &= \frac{\Gamma_1 \Delta y_j}{4\pi} \left[\frac{z}{(y'^2 + z^2)} + \frac{z}{(y''^2 + z^2)} \right] \\ &+ \frac{\Gamma_2 \Delta y_j}{4\pi} \left[\frac{1}{\sqrt{x'^2 + (y'^2 + z^2)^2} (y'^2 + z^2)} + \frac{1}{\sqrt{x''^2 + (y''^2 + z^2)^2} (y''^2 + z^2)} \right] z x' \quad (C-3) \end{aligned}$$

where, the above equation was normalized by using,

$$\tau_1 = \frac{\Gamma_1}{U_0 b}, \quad (\Phi_m)_j = \frac{(\bar{\Phi}_m)_j}{U_0 b}, \quad \Delta y_j = \frac{\Delta y_j}{b}$$

$$y' = \frac{y-y_j}{b}, \quad y'' = \frac{y+y_j}{b}, \quad z = \frac{z}{b}$$

$$\text{and } x' = \frac{x-x_j}{b\rho} \quad (C-4)$$

APPENDIX C

In this appendix the transform of the velocity potential of the model, and its y and z derivatives are evaluated. The velocity potential of the horse shoe vortex at the origin is given by,

$$\Phi_m = \frac{\Gamma S}{2\pi} \left[1 + \frac{x}{\sqrt{x^2 + \beta^2(y^2 + z^2)}} \right] \left[\frac{z}{y^2 + z^2} \right] \quad (C-1)$$

where S is the half span.

If we consider the model as made up of pairs of elements, then for an element pair j of span Δy_j which is located at $x = \pm x_j$, $y = y_j$ the model potential is given by equation (C-2). The lifting element is shown in Fig. 12.

$$\begin{aligned} (\Phi_m)_j &= \frac{\Gamma_j \Delta y_j}{4\pi} \left[1 + \frac{(x - x_j)}{\sqrt{(x - x_j)^2 + \beta^2[(y - y_j)^2 + z^2]}} \right] \left[\frac{z}{(y - y_j)^2 + z^2} \right] \\ &+ \frac{\Gamma_j \Delta y_j}{4\pi} \left[1 + \frac{x - x_j}{\sqrt{(x - x_j)^2 + \beta^2[(y + y_j)^2 + z^2]}} \right] \left[\frac{z}{(y + y_j)^2 + z^2} \right]. \end{aligned} \quad (C-2)$$

In normalized form this model potential can be written as,

$$\begin{aligned} (\phi_m)_j &= \frac{\sigma_j \Delta y_j}{4\pi} \left[\frac{z}{(y'^2 + z^2)} + \frac{z}{(y''^2 + z^2)} \right] \\ &+ \frac{\sigma_j \Delta y_j}{4\pi} \left[\frac{1}{\sqrt{x'^2 + (y'^2 + z^2)} (y'^2 + z^2)} + \frac{1}{\sqrt{x'^2 + (y''^2 + z^2)} (y''^2 + z^2)} \right] z x' \end{aligned} \quad (C-3)$$

where, the above equation was normalized by using,

$$\sigma_j = \frac{\Gamma_j}{U_\infty b}, \quad (\phi_m)_j = \frac{(\Phi_m)_j}{U_\infty b}, \quad \Delta y_j = \frac{\Delta y_j}{b}$$

$$y' = \frac{y - y_j}{b}, \quad y'' = \frac{y + y_j}{b}, \quad z = \frac{z}{b}$$

and $x' = \frac{x - x_j}{b\beta}$. (C-4)

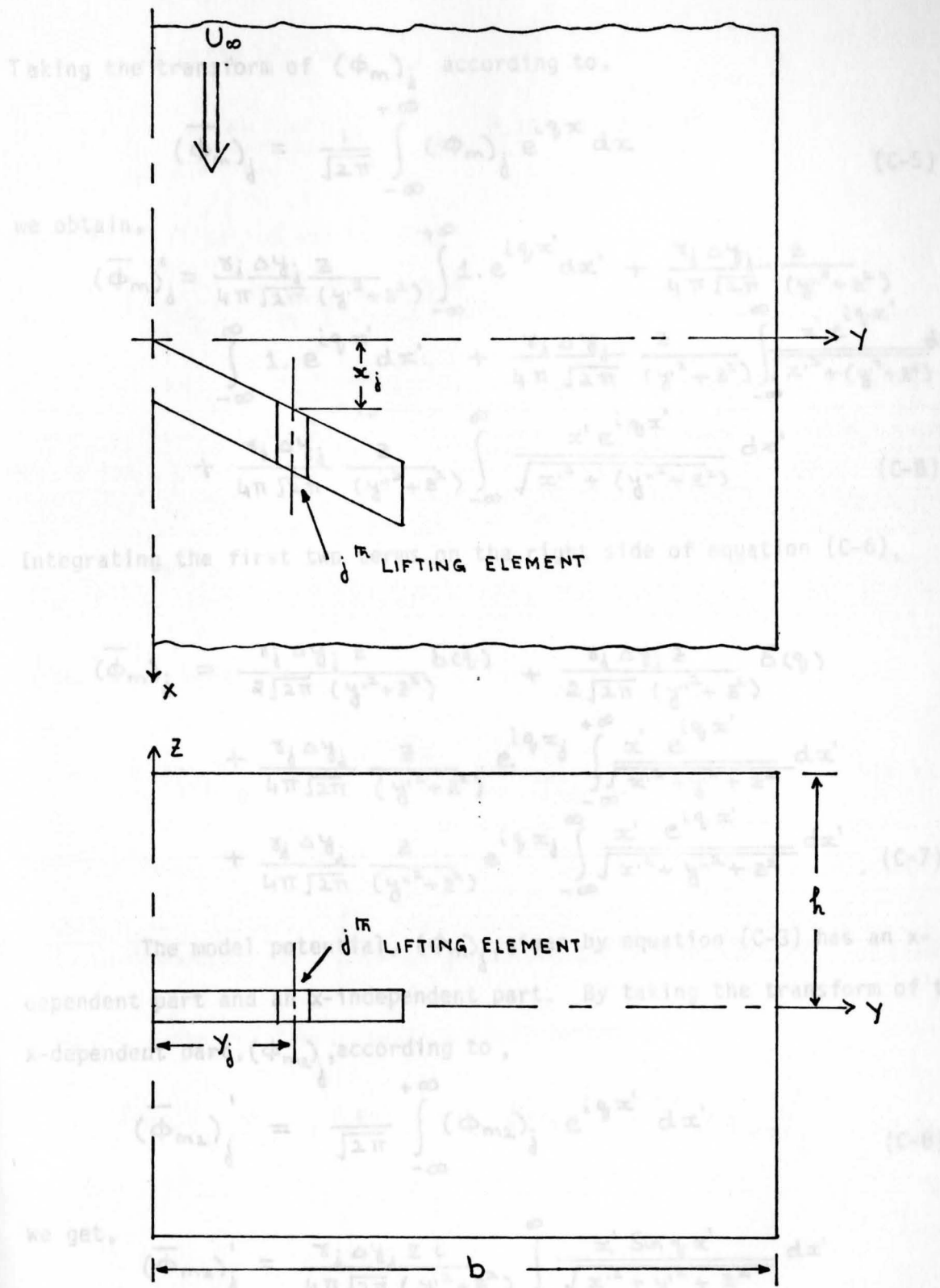


Fig. 12. Location of The Lifting Element

The Cos part of equation (C-8) is zero since $(\phi_{m2})_j$ is an odd function

Taking the transform of $(\Phi_m)_j$ according to,

$$(\bar{\Phi}_m)_j = \frac{1}{\sqrt{2\pi}} \int_{-\infty}^{+\infty} (\Phi_m)_j e^{iqx} dx \quad (C-5)$$

we obtain,

$$\begin{aligned} (\bar{\Phi}_m)_j' &= \frac{\gamma_j \Delta y_j z}{4\pi \sqrt{2\pi} (y_j^2 + z^2)} \int_{-\infty}^{+\infty} 1 \cdot e^{iqx'} dx' + \frac{\gamma_j \Delta y_j z}{4\pi \sqrt{2\pi} (y_j^2 + z^2)} \\ &\int_{-\infty}^{\infty} 1 \cdot e^{iqx'} dx' + \frac{\gamma_j \Delta y_j z}{4\pi \sqrt{2\pi} (y_j^2 + z^2)} \int_{-\infty}^{\infty} \frac{x' e^{iqx'}}{\sqrt{x'^2 + (y_j^2 + z^2)}} dx' \\ &+ \frac{\gamma_j \Delta y_j z}{4\pi \sqrt{2\pi} (y_j^2 + z^2)} \int_{-\infty}^{\infty} \frac{x' e^{iqx'}}{\sqrt{x'^2 + (y_j^2 + z^2)}} dx'. \end{aligned} \quad (C-6)$$

Integrating the first two terms on the right side of equation (C-6),

$$\begin{aligned} (\bar{\Phi}_m)_j &= \frac{\gamma_j \Delta y_j z}{2\sqrt{2\pi} (y_j^2 + z^2)} \delta(q) + \frac{\gamma_j \Delta y_j z}{2\sqrt{2\pi} (y_j^2 + z^2)} \delta(q) \\ &+ \frac{\gamma_j \Delta y_j z}{4\pi \sqrt{2\pi} (y_j^2 + z^2)} e^{iqx_j} \int_{-\infty}^{+\infty} \frac{x' e^{iqx'}}{\sqrt{x'^2 + y_j^2 + z^2}} dx' \\ &+ \frac{\gamma_j \Delta y_j z}{4\pi \sqrt{2\pi} (y_j^2 + z^2)} e^{iqx_j} \int_{-\infty}^{\infty} \frac{x' e^{iqx'}}{\sqrt{x'^2 + y_j^2 + z^2}} dx'. \end{aligned} \quad (C-7)$$

The model potential, $(\Phi_m)_j$, given by equation (C-3) has an x-dependent part and an x-independent part. By taking the transform of the x-dependent part, $(\Phi_{m_2})_j$, according to,

$$(\bar{\Phi}_{m_2})_j' = \frac{1}{\sqrt{2\pi}} \int_{-\infty}^{+\infty} (\Phi_{m_2})_j e^{iqx'} dx' \quad (C-8)$$

we get,

$$\begin{aligned} (\bar{\Phi}_{m_2})_j' &= \frac{\gamma_j \Delta y_j z i}{4\pi \sqrt{2\pi} (y_j^2 + z^2)} \int_{-\infty}^{\infty} \frac{x' \sin qx'}{\sqrt{x'^2 + y_j^2 + z^2}} dx' \\ &+ \frac{\gamma_j \Delta y_j z i}{4\pi \sqrt{2\pi} (y_j^2 + z^2)} \int_{-\infty}^{+\infty} \frac{x' \sin qx'}{\sqrt{x'^2 + y_j^2 + z^2}} dx'. \end{aligned} \quad (C-9)$$

The Cos part of equation (C-8) is zero since $(\Phi_{m_2})_j$ is an odd function

of x' . By using the relation,

$$\int_{-\infty}^{+\infty} \frac{x \sin qx}{\sqrt{x^2 + 1}} dx = \frac{2q}{|q|} K_1(|q|) \quad (C-10)$$

equation (C-9) can be written as,

$$\begin{aligned} (\bar{\Phi}_{m_2})'_j &= \frac{\sigma_j \Delta y_j z q i}{|q| 2\pi \sqrt{2\pi} \sqrt{y'^2 + z^2}} K_1(|q| \sqrt{y'^2 + z^2}) \\ &+ \frac{\sigma_j \Delta y_j z q i}{|q| 2\pi \sqrt{2\pi} \sqrt{y''^2 + z^2}} K_1(|q| \sqrt{y''^2 + z^2}) \end{aligned} \quad (C-11)$$

Noting that,

$$(\bar{\Phi}_{m_2})'_j = \frac{1}{\sqrt{2\pi}} \int_{-\infty}^{+\infty} e^{iqx} (\Phi_{m_2})_j e^{-iqx_j} dx \quad (C-12)$$

which can be written as,

$$(\bar{\Phi}_{m_2})'_j = e^{-iqx_j} (\bar{\Phi}_{m_2})_j \quad (C-13)$$

Hence, $(\bar{\Phi}_{m_2})_j$ is given by

$$(\bar{\Phi}_{m_2})_j = \left[\cos qx_j + i \sin qx_j \right] (\bar{\Phi}_{m_2})'_j \quad (C-14)$$

Using the above relation, equation (C-7) becomes,

$$(\bar{\Phi}_m)_j = c_1 \delta(q) + c_2 \delta(q) + e^{iqx_j} (\bar{\Phi}_{m_2})'_j \quad (C-15)$$

where,

$$c_1 = \frac{\sigma_j \Delta y_j z}{2\sqrt{2\pi} (y'^2 + z^2)} \quad (C-16)$$

$$c_2 = \frac{\sigma_j \Delta y_j z}{2\sqrt{2\pi} (y''^2 + z^2)} \quad (C-17)$$

Substituting the value of $(\bar{\Phi}_{m2})_j$ from equation (C-11) in equation (C-15) we get,

$$(\bar{\Phi}_m)_j = (c_1 \delta(\varrho) + c_2 \delta(\varrho)) - \frac{\gamma_j \Delta y_j z \varrho \sin \varrho x_j}{2\pi \sqrt{2\pi} |y|} \\ + \frac{\gamma_j \Delta y_j z \varrho \cos \varrho x_j}{2\pi \sqrt{2\pi} |y|} \left[\frac{K_1(|y| \sqrt{y'^2 + z^2})}{\sqrt{y'^2 + z^2}} + \frac{K_1(|y| \sqrt{y''^2 + z^2})}{\sqrt{y''^2 + z^2}} \right] \\ + \frac{\gamma_j \Delta y_j z \varrho \cos \varrho x_j}{2\pi \sqrt{2\pi} |y|} \left[\frac{K_1(|y| \sqrt{y'^2 + z^2})}{\sqrt{y'^2 + z^2}} + \frac{K_1(|y| \sqrt{y''^2 + z^2})}{\sqrt{y''^2 + z^2}} \right] i \quad (C-18)$$

In the above equation, if the real part which is independent of $\delta(\varrho)$ is denoted by M_{1R} and the imaginary part by M_{1i} then equation (C-18) becomes,

$$(\bar{\Phi}_m)_j = M_{1R} + (c_1 + c_2) \delta(\varrho) + i M_{1i} \quad (C-19)$$

Derivatives of the Model Potential

The derivatives of the transform of the model potential, $(\bar{\Phi}_m)$, with respect to y and z are given below. The derivatives of the real and the imaginary part are taken separately.

Derivative With Respect To y

Real Part

The derivative of the real part of equation (C-19) is given by,

$$\frac{\partial}{\partial y} \left[M_{1R} + (c_1 + c_2) \delta(\varrho) \right] = \frac{-\gamma_j \Delta y_j z}{2 \sqrt{2\pi}} \frac{2y'}{(y'^2 + z^2)^2} \delta(\varrho) \\ - \frac{\gamma_j \Delta y_j z}{2 \sqrt{2\pi}} \frac{2y''}{(y''^2 + z^2)^2} \delta(\varrho) + \frac{\gamma_j \Delta y_j z \varrho}{2\pi \sqrt{2\pi}} \sin \varrho x_j \\ \left[\frac{|y| y' K_0(|y| \sqrt{y'^2 + z^2})}{(y'^2 + z^2)} + \frac{2y' K_1(|y| \sqrt{y'^2 + z^2})}{(y'^2 + z^2)^{3/2}} \right] \\ + \frac{|y| y'' K_0(|y| \sqrt{y''^2 + z^2})}{(y''^2 + z^2)} + \frac{2y'' K_1(|y| \sqrt{y''^2 + z^2})}{(y''^2 + z^2)^{3/2}} \quad (C-20)$$

The above equation can be represented by,

$$\frac{\partial}{\partial y} \left[M_{1R} + (c_1 + c_2) \delta(\varphi) \right] = M_{2R} + \xi \delta(\varphi) \quad (C-21)$$

where, M_{2R} represents the part of the equation (C-21) which is independent of $\delta(\varphi)$. The coefficient of $\delta(\varphi)$ part of equation (C-21) is represented by ξ .

Imaginary Part

The derivative of the imaginary part of equation (C-19) is given by,

$$\begin{aligned} \frac{\partial}{\partial y} M_{ii} = & \frac{\delta_j \Delta y_j z \varphi \cos \varphi x_j}{2\pi \sqrt{2\pi} |y|} \left[\frac{|y| y' K_0(|y| \sqrt{y'^2 + z^2})}{(y'^2 + z^2)} \right. \\ & + \frac{2 y' K_1(|y| \sqrt{y'^2 + z^2})}{(y'^2 + z^2)^{3/2}} + \frac{|y| y'' K_0(|y| \sqrt{y''^2 + z^2})}{(y''^2 + z^2)} \\ & \left. + \frac{2 y'' K_1(|y| \sqrt{y''^2 + z^2})}{(y''^2 + z^2)^{3/2}} \right] \end{aligned} \quad (C-22)$$

If the right hand side of the above equation is represented by M_{2i} , then,

$$\frac{\partial}{\partial y} M_{ii} = M_{2i} \quad (C-23)$$

Combining the real and the imaginary part, the y derivative of the transform of the model potential of an element j is given by,

$$\frac{\partial}{\partial y} (\bar{\Phi}_m)_j = M_{2R} + \xi \delta(\varphi) + i M_{2i} \quad (C-24)$$

Derivative With Respect to z

Real Part

The derivative of the real part of equation (C-19) is given by,

$$\begin{aligned}
\frac{\partial}{\partial z} (M_{1R} + (C_1 + C_2) \delta(\varrho)) &= \frac{\sigma_j \Delta y_j}{2 \sqrt{2\pi}} \left[\frac{(y'^2 + z^2) - 2z^2}{(y'^2 + z^2)^2} \right] \delta(\varrho) \\
&+ \frac{\sigma_j \Delta y_j}{2 \sqrt{2\pi}} \left[\frac{(y''^2 + z^2) - 2z^2}{(y''^2 + z^2)} \right] \delta(\varrho) \\
&+ \frac{\sigma_j \Delta y_j \varrho \sin \varrho x_j}{2\pi \sqrt{2\pi} \varrho} \left[\left(\frac{2z^2}{y'^2 + z^2} - 1 \right) \frac{K_1(1\varrho \sqrt{y'^2 + z^2})}{\sqrt{y'^2 + z^2}} + \right. \\
&\frac{1\varrho z^2 K_0(1\varrho \sqrt{y'^2 + z^2})}{(y'^2 + z^2)} + \left. \left(\frac{2z^2}{y''^2 + z^2} - 1 \right) \frac{K_1(1\varrho \sqrt{y''^2 + z^2})}{\sqrt{y''^2 + z^2}} + \right. \\
&\left. \left. + \frac{1\varrho z^2 K_0(1\varrho \sqrt{y''^2 + z^2})}{(y''^2 + z^2)} \right] \right]. \quad (C-25)
\end{aligned}$$

If M_{3R} represents the part of the equation (C-25) which is independent of $\delta(\varrho)$ and the coefficient of the $\delta(\varrho)$ part of the equation is,

$$\frac{\partial}{\partial z} [M_{1R} + (C_1 + C_2) \delta(\varrho)] = M_{3R} + \nu \delta(\varrho). \quad (C-26)$$

Imaginary Part

The derivative of the imaginary part of equation ((C-19) is given by,

$$\begin{aligned}
\frac{\partial}{\partial z} M_{ii} &= \frac{-\sigma_j \Delta y_j \varrho \cos \varrho x_j}{2\pi \sqrt{2\pi} \varrho} \left[\left(\frac{2z^2}{y'^2 + z^2} - 1 \right) \right. \\
&\frac{K_1(1\varrho \sqrt{y'^2 + z^2})}{\sqrt{y'^2 + z^2}} + \frac{1\varrho z^2 K_0(1\varrho \sqrt{y'^2 + z^2})}{(y'^2 + z^2)} \\
&\left. + \left(\frac{2z^2}{y''^2 + z^2} - 1 \right) \frac{K_1(1\varrho \sqrt{y''^2 + z^2})}{\sqrt{y''^2 + z^2}} + \frac{1\varrho z^2 K_0(1\varrho \sqrt{y''^2 + z^2})}{(y''^2 + z^2)} \right]. \quad (C-27)
\end{aligned}$$

Representing the right hand side of the above equation by M_{3i} ,

$$\frac{\partial}{\partial z} (M_{ii}) = M_{3i} \quad (C-28)$$

Combining the real and the imaginary part, the z-derivative of the transform of the model potential of an element j is given by,

$$\frac{\partial}{\partial z} (\bar{\Phi}_m)_j = M_{3R} + M_{3i} + \nu \delta(\rho_j) \quad (C-29)$$

The term $W_j(n, q)$ is given by equation (B-50) in appendix B. The value of $W_j(n, q)$ is different for each of the wall elements and for each value of q . These values of $W_j(n, q)$ can be expressed by a column matrix,

$$\{W_j\} = \{T\} \{r\} \quad (D-1)$$

For $k \leq k_1$, the nk^{th} element of matrix $\{T\}$ is obtained by using equation (B-49) in appendix B. The matrix $\{T\}$ for this case is,

$$\begin{aligned} \{T\}_{nk} = & F_1 \left[2|r_1|, |r_1|(\bar{z}_n - z_{k+1}), |r_1|(\bar{z}_n - z_n) \right] \\ & - F_1 \left[2|r_1|, |r_1|(\bar{z}_n + z_n), |r_1|(\bar{z}_n + z_{k+1}) \right] \\ & + \begin{bmatrix} \pi & \text{if } k = n \\ 0 & \text{if } k \neq n \end{bmatrix} \quad (D-2) \end{aligned}$$

The terms in the above equation are for the left wall top half, left wall bottom half and the right wall.

For $k_1 < k \leq k_2$ the value of the nk^{th} element of matrix $\{T\}$ is given by,

$$\{T\}_{nk} = F_2 \left[|r_1|(\bar{z}_n - \gamma_0), |r_1|(1 - \gamma_{k+1}), |r_1|(1 - \gamma_n) \right]$$

APPENDIX D

The terms used in the boundary condition equations are described in this appendix in a matrix form. These terms are given below.

Matrix Expression for $W_1^i(n,q)$ and $W_1''(n,q)$

The term $W_1(n,q)$ is given by equation (B-50) in appendix B. The value of $W_1(n,q)$ is different for each of the wall elements and for each value of q . These values of $W_1(n,q)$ can be expressed by a column matrix,

$$\{W_1\} = \{T\} \{\sigma\} \quad (D-1)$$

For $k \leq k_1$, the nk^{th} element of matrix $\{T\}$ is obtained by using equation (B-49) in appendix B. The matrix $\{T\}$ for this case is,

$$\begin{aligned} \{T\}_{nk} = & F_1 \left[2|q|, |q|(\bar{z}_n - z_{k+1}), |q|(\bar{z}_n - z_k) \right] \\ & - F_1 \left[2|q|, |q|(\bar{z}_n + z_k), |q|(\bar{z}_n + z_{k+1}) \right] \\ & + \begin{bmatrix} \pi & 1F & k = n \\ 0 & 1F & k \neq n \end{bmatrix} \end{aligned} \quad (D-2)$$

The terms in the above equation are for the left wall top half, left wall bottom half and the right wall.

For $k_1 < k \leq k_2$ the value of the nk^{th} element of matrix $\{T\}$ is given by,

$$\{T\}_{nk} = F_2 \left[|q|(\bar{z}_n - r/b), |q|(1 - \gamma_{k+1}), |q|(1 - \gamma_k) \right]$$

$$\begin{aligned}
& + F_2 \left[|v| (\bar{z}_n - r/b), |v| (1 + \gamma_k), |v| (1 + \gamma_{k+1}) \right] \\
& - F_2 \left[|v| (\bar{z}_n + r/b), |v| (1 - \gamma_{k+1}), |v| (1 - \gamma_k) \right] \\
& - F_2 \left[|v| (\bar{z}_n + r/b), |v| (1 + \gamma_k), |v| (1 + \gamma_{k+1}) \right] .
\end{aligned} \tag{D-3}$$

The terms in the above equation are for the top wall right half, top wall left half, bottom wall right half and the bottom wall left half respectively. In equation (D-2) and equation (D-3), n may take on index values from 1 to k_1 . Some values of n correspond to the solid elements and others to slotted wall elements. It is convenient to define $\{T\}_{y \text{ slot}}$ and $\{T\}_{y \text{ solid}}$ such that the former is $\{T\}$ for the set of slotted wall element indices and the latter is $\{T\}$ for the set of solid element indices located at $y = 1$. The matrices $\{W_1'\}$ and $\{W_1''\}$ can be obtained by putting the real and the imaginary values of σ . Thus,

$$\{W_1'\} = \{T\} \{\sigma'\} \tag{D-4}$$

$$\{W_1''\} = \{T\} \{\sigma''\} . \tag{D-5}$$

Matrix Expression For $W_2'(n,q)$ and $W_2''(n,q)$

The term $W_2(n,q)$ is given by equation (B-55) in appendix B. The value of $W_2(n,q)$ is different for each wall element and for each value of q . These values can be expressed in a matrix form by putting,

$$W_2(n,q) = \{U\} \{\sigma\} . \tag{D-6}$$

For $K_1 < k \leq K_2$ the nk^{th} element of the matrix $\{U\}$ is given by,

$$\{U\}_{nk} = - \begin{bmatrix} F_1 & 2i\eta_1 \frac{h}{b}, i\eta_1 (\bar{y}_n - y_{k+1}), i\eta_1 (\bar{y}_n - y_k) \\ F_1 & 2i\eta_1 \frac{h}{b}, i\eta_1 (\bar{y}_n + y_k), i\eta_1 (\bar{y}_n + y_{k+1}) \end{bmatrix} \begin{bmatrix} \pi & \text{IF } k = n \\ 0 & \text{IF } k \neq n \end{bmatrix} \quad (D-7)$$

The first two terms in the above equation are due to the bottom wall and the last two terms are due to the top wall.

For $k \leq K_1$ the nk^{th} element of matrix $\{U\}$ is,

$$\{U\}_{nk} = F_2 \begin{bmatrix} i\eta_1 (\bar{y}_n + 1), i\eta_1 (h/b - z_{k+1}), i\eta_1 (h/b - z_k) \\ i\eta_1 (\bar{y}_n + 1), i\eta_1 (h/b + z_k), i\eta_1 (h/b + z_{k+1}) \\ i\eta_1 (\bar{y}_n - 1), i\eta_1 (h/b - z_{k+1}), i\eta_1 (h/b - z_k) \\ i\eta_1 (\bar{y}_n - 1), i\eta_1 (h/b + z_k), i\eta_1 (h/b + z_{k+1}) \end{bmatrix} \quad (D-8)$$

The terms in the above equation are due to the left wall top half, left wall bottom half, right wall top half and the right wall bottom half respectively.

In equation (D-7) and equation (D-8), n takes on values from $K_1 + 1$ to K_2 . Some values of n correspond to solid elements and some to the slotted elements. We define matrices $\{U\}_z \text{ slot}$ and $\{U\}_z \text{ solid}$ such that the former matrix is for the set of slotted element and the latter matrix is for the set of solid elements. The value of $\{W'_2\}$ and $\{W''_2\}$ can be obtained by putting the real and the imaginary values of the influence coefficient in equation (D-6). Hence,

$$\{W'_2\} = \{U\} \{\sigma'\} \quad (D-9)$$

$$\{W''_2\} = \{U\} \{\sigma''\} \quad (D-10)$$

Matrix Expression for $W_3^I(n,q)$ and $W_3^{II}(n,q)$

The function $W_3(n,q)$ is defined by equation (A-41) in appendix A. $W_3(n,q)$ has a different value for each n^{th} wall element and for each value of q . For each q , it is convenient to express the values of $W_3(n,q)$ as elements of a column matrix.

$$\{W_3\} = \{c\} \{\sigma\} \quad (D-11)$$

The matrix $\{\sigma\}$ is a column matrix of K_2 elements and $\{c\}$ is a $(K_1 - N_1)$ by K_2 matrix. The nk^{th} element of $\{c\}$ can be found by using equation (A-40) and equation (A-41) of appendix A. For $k \leq K_1$, the nk^{th} element is given by,

$$\begin{aligned} \{c\}_{nk} = & G_1 \left[2|q|, |q| (\bar{z}_n - z_{k+1}), |q| (\bar{z}_n - z_k) \right] \\ & - G_1 \left[2|q|, |q| (\bar{z}_n + z_k), |q| (\bar{z}_n + z_{k+1}) \right] \\ & - G_1 \left[0, |q| (\bar{z}_n + z_k), |q| (\bar{z}_n + z_{k+1}) \right] \\ & \left[G_1 \left[0, |q| (\bar{z}_n - z_{k+1}), |q| (\bar{z}_n - z_k) \right] \text{ IF } n \neq k \right. \\ & \left. - 2G_1 \left[0, \frac{|q|}{2} (z_{k+1} - z_k), 0 \right] \text{ IF } n = k \right] \quad (D-12) \end{aligned}$$

The terms on the right hand side of equation (D-12) are for the left wall top half, left wall bottom half, right wall bottom half and the right wall top half.

The nk^{th} element of matrix $\{c\}$ for $K_1 < k \leq K_2$ is given by,

$$\begin{aligned} \{c\}_{nk} = & G_1 \left[|q| (\bar{z}_n - R/b), |q| (1 - \gamma_{k+1}), |q| (1 - \gamma_k) \right] \\ & + G_1 \left[|q| (\bar{z}_n - R/b), |q| (1 + \gamma_k), |q| (1 + \gamma_{k+1}) \right] \\ & - G_1 \left[|q| (\bar{z}_n + \frac{b}{2}), |q| (1 - \gamma_{k+1}), |q| (1 - \gamma_k) \right] \\ & - G_1 \left[|q| (\bar{z}_n + R/b), |q| (1 + \gamma_k), |q| (1 + \gamma_{k+1}) \right] \quad (D-13) \end{aligned}$$

The terms on the right hand side of the above equation are for the top wall right half, top wall left half, bottom wall right half and the bottom wall left half. In equation (D-12) and equation (D-13), n takes on values only corresponding to the slotted element index numbers on $y = 1$. If prime and double prime denotes the real and the imaginary part of the influence coefficient, then we can express it as,

$$\sigma = \sigma' + i \sigma'' \quad (D-14)$$

Therefore,

$$\{W_3\} = \{c\} \left[\{\sigma'\} + i \{\sigma''\} \right] \quad (D-15)$$

Hence the real and the imaginary part of $\{W_3\}$ are,

$$\{W_3'\} = \{c\} \{\sigma'\} \quad (D-16)$$

$$\{W_3''\} = \{c\} \{\sigma''\} \quad (D-17)$$

Matrix Expression For $W_4'(n,q)$ and $W_4''(n,q)$

The function $W_4(n,q)$ is defined by equation (A-45) in appendix A. The value of $W_4(n,q)$ is different for each n^{th} wall element and for each value of q . For each value of q , the column matrix can be expressed as,

$$\{W_4\} = \{D\} \{\sigma\} \quad (D-18)$$

For $k \leq K_1$ the nk^{th} element of the matrix $\{D\}$ is given by,

$$\{D\}_{nk} = G_1 \left[|v_1(\bar{y}_n + 1)|, |v_1(R/b - z_{k+1})|, |v_1(R/b - z_k)| \right]$$

$$\begin{aligned}
& - G_1 \left[191 (\bar{y}_n + 1), 191 (h/b + z_{k+1}), 191 (h/b + z_k) \right] \\
& + G_1 \left[191 (\bar{y}_n - 1), 191 (h/b - z_{k+1}), 191 (h/b - z_k) \right] \\
& - G_1 \left[191 (\bar{y}_n - 1), 191 (h/b + z_{k+1}), 191 (h/b + z_k) \right] .
\end{aligned} \tag{D-19}$$

The right hand terms in the above equation are due to the left wall top half, left wall bottom half, right wall top half and the right wall bottom half respectively.

For $K_1 < k \leq K_2$ the nk^{th} element of the matrix $\{D\}$ is given by,

$$\begin{aligned}
\{D\}_{nk} = & G_1 \left[0, 191 (\bar{y}_n + y_{k+1}), 191 (\bar{y}_n + y_k) \right] \\
& - G_1 \left[2 h/b 191, 191 (\bar{y}_n - y_{k+1}), 191 (\bar{y}_n - y_k) \right] \\
& - G_1 \left[2 h/b 191, 191 (\bar{y}_n + y_{k+1}), 191 (\bar{y}_n + y_k) \right] \\
& + \left[\begin{array}{l} G_1 \left[0, 191 (\bar{y}_n - y_{k+1}), 191 (\bar{y}_n - y_k) \right] \text{ if } n \neq k \\ -2G_1 \left[0, \frac{191}{2} (y_{k+1} - y_k), 0 \right] \text{ if } n = k \end{array} \right] \tag{D-20}
\end{aligned}$$

The terms in the above equation are due to the top wall left half, bottom wall right half, bottom wall left half and the top wall right half respectively. In equation (D-19) and equation (D-20) n takes on values only corresponding to the slotted element index numbers on $z = h/b$. The matrices $\{W'_4\}$ and $\{W''_4\}$ are obtained by putting the real and the imaginary values of the influence coefficient. Thus,

$$\{W'_4\} = \{D\} \{\sigma'\} \tag{D-21}$$

$$\{W''_4\} = \{D\} \{\sigma''\} . \tag{D-22}$$

Matrix Expression For M_{1i} and M_{1r}

The term M_{1i} is the imaginary part of equation (C-18). It is given by,

$$M_{1i} = \frac{\sigma_j \Delta y_j z q \cos q x_j}{2\pi \sqrt{2\pi} |q|} \left\{ \frac{K_1 (|q| \sqrt{y_j'^2 + z^2})}{\sqrt{y_j'^2 + z^2}} + \frac{K_1 (|q| \sqrt{y_j''^2 + z^2})}{\sqrt{y_j''^2 + z^2}} \right\} \quad (D-23)$$

The above equation is a function of q and n . Therefore,

$$M_{1iL} = M_{1i}(n, q) \quad (D-24)$$

The function $M_{1i}(n, q)$ has a different value for each wall element and for each value of q . For a fixed q , we can represent $M_{1i}(n, q)$ by a $(K_2 \times 1)$ matrix. K_2 is the total number of wall elements. Therefore,

$$\{M_{1i}\} = \begin{bmatrix} (M_{1i})_{11} \\ (M_{1i})_{21} \\ (M_{1i})_{31} \\ \vdots \\ (M_{1i})_{K_2 1} \end{bmatrix} \quad (D-25)$$

The term M_{1r} is the real part of equation (C-18). It does not contain the $\delta(q)$ part and is given by,

$$M_{1r} = \frac{-\sigma_j \Delta y_j z q \sin q x_j}{2\pi \sqrt{2\pi} |q|} \left\{ \frac{K_1 (|q| \sqrt{y_j'^2 + z^2})}{\sqrt{y_j'^2 + z^2}} + \frac{K_1 (|q| \sqrt{y_j''^2 + z^2})}{\sqrt{y_j''^2 + z^2}} \right\} \quad (D-26)$$

The above equation is a function of q and n . Therefore,

$$M_{1rL} = M_{1r}(n, q) \quad (D-27)$$

The value of n varies for each wall element. For K_2 wall elements and a fixed q the function $M_{1R}(n, q)$ can be represented by a $(K_2 \times 1)$ matrix. Hence the matrix $\{M_{1R}\}$ is,

$$\{M_{1R}\} = \begin{bmatrix} (M_{1R})_{11} \\ (M_{1R})_{21} \\ \vdots \\ (M_{1R})_{K_2 1} \end{bmatrix} \quad (D-28)$$

Matrix Expression for M_{2R} and M_{2i}

The term M_{2R} is the $\delta(q)$ independent part of equation (C-22).

M_{2R} is given by,

$$M_{2R} = \frac{\tau_i \Delta y_i z q \sin q x_i}{2\pi \sqrt{2\pi} 191} \left\{ \frac{191 y' K_0 (191 \sqrt{y'^2 + z^2})}{(y'^2 + z^2)} + \frac{2 y' K_1 (191 \sqrt{y'^2 + z^2})}{(y'^2 + z^2)^{3/2}} + \frac{191 y'' K_0 (191 \sqrt{y''^2 + z^2})}{(y''^2 + z^2)} + \frac{2 y'' K_1 (191 \sqrt{y''^2 + z^2})}{(y''^2 + z^2)^{3/2}} \right\} \quad (D-29)$$

Since z is a function of n , M_{2R} is also a function of n . Hence, the above equation can be written as,

$$M_{2R} = M_{2R}(n, q) \quad (D-30)$$

For a fixed q , the values of $M_{2R}(n, q)$ for each wall element can be expressed by a matrix $\{M_{2R}\}$. If K_2 is the total number of wall element, the matrix $\{M_{2R}\}$ is a column matrix of the order $(K_2 \times 1)$.

$$\{M_{2R}\} = \begin{bmatrix} (M_{2R})_{11} \\ (M_{2R})_{21} \\ \vdots \\ (M_{2R})_{k_{21}} \end{bmatrix} \quad (D-31)$$

The function M_{2i} is obtained by differentiating M_{1i} with respect to y . The equation for M_{2i} is,

$$M_{2i} = \frac{-\delta_i \Delta y_i z q \cos \alpha_i}{2\pi \sqrt{2\pi} 191} \left[\frac{191 y' K_0(191 \sqrt{y'^2 + z^2})}{(y'^2 + z^2)} + \frac{2y' K_1(191 \sqrt{y'^2 + z^2})}{(y'^2 + z^2)^{3/2}} + \frac{191 y'' K_0(191 \sqrt{y''^2 + z^2})}{(y''^2 + z^2)} + \frac{2y'' K_1(191 \sqrt{y''^2 + z^2})}{(y''^2 + z^2)^{3/2}} \right] \quad (D-32)$$

The above equation is a function of z and q . Since z is a function of n , we can express equation (D-32) as,

$$M_{2i} = M_{2i}(n, q) \quad (D-33)$$

$M_{2i}(n, q)$ has a different value for each of the wall elements and for each value of q . For a constant q and all the K_2 elements we can represent the values of $M_{2i}(n, q)$ by a column matrix $\{M_{2i}\}$.

$$\{M_{2i}\} = \begin{bmatrix} (M_{2i})_{11} \\ (M_{2i})_{21} \\ \vdots \\ (M_{2i})_{k_{21}} \end{bmatrix} \quad (D-34)$$

Matrix Expression for M_{3R} and M_{3i}

The term M_{3R} is the $\delta(q)$ independent part of equation (C-25).

It is given by,

$$\begin{aligned}
 M_{3R} = & \frac{\tau_j \Delta y_j q \sin q x_j}{2\pi \sqrt{2\pi} |q|} \left[\left(\frac{2z^2}{y'^2 + z^2} - 1 \right) \frac{K_1(|q| \sqrt{y'^2 + z^2})}{\sqrt{y'^2 + z^2}} \right. \\
 & + \frac{|q| z^2 K_0(|q| \sqrt{y'^2 + z^2})}{(y'^2 + z^2)} + \left. \left(\frac{2z^2}{y''^2 + z^2} - 1 \right) \frac{K_1(|q| \sqrt{y''^2 + z^2})}{\sqrt{y''^2 + z^2}} \right. \\
 & \left. + \frac{|q| z^2 K_0(|q| \sqrt{y''^2 + z^2})}{(y''^2 + z^2)} \right] \quad (D-35)
 \end{aligned}$$

The above equation is a function of n and q . Therefore we can express it as,

$$M_{3R} = M_{3R}(n, q) \quad (D-36)$$

The function $M_{3R}(n, q)$ has a different value for each wall element and for each value of q . For each q , we can express K_2 values of M_{3R} by a column matrix $\{M_{3R}\}$. Where,

$$\{M_{3R}\} = \begin{bmatrix} (M_{3R})_{11} \\ (M_{3R})_{21} \\ \vdots \\ (M_{3R})_{K_2 1} \end{bmatrix} \quad (D-37)$$

The function M_{3i} is obtained by differentiating M_{1i} with respect to z . It is given by,

$$M_{3i} = \frac{-\tau_j \Delta y_j q \cos q x_j}{2\pi \sqrt{2\pi} |q|} \left[\left(\frac{2z^2}{y'^2 + z^2} - 1 \right) \right]$$

$$\begin{aligned}
& \frac{K_1 (191 \sqrt{y'^2 + z^2})}{\sqrt{y'^2 + z^2}} + \frac{191 z^2 K_0 (191 \sqrt{y'^2 + z^2})}{(y'^2 + z^2)} \\
& + \left(\frac{2 z^2}{y''^2 + z^2} - 1 \right) \frac{K_1 (191 \sqrt{y''^2 + z^2})}{\sqrt{y''^2 + z^2}} \\
& + \frac{191 z^2 K_0 (191 \sqrt{y''^2 + z^2})}{(y''^2 + z^2)} \Bigg] . \tag{D-38}
\end{aligned}$$

The above equation can be expressed as a function of n and q . That is,

$$M_{3i} = M_{3i}(n, q) . \tag{D-39}$$

The function $M_{3i}(n, q)$ has a different value for each wall element and for each value of q . For each q , we can express K_2 values of M_{3i} by a column matrix, $\{M_{3i}\}$. Where,

$$\{M_{3i}\} = \begin{bmatrix} (M_{3i})_{11} \\ (M_{3i})_{21} \\ \vdots \\ (M_{3i})_{k21} \end{bmatrix} \tag{D-40}$$

Matrix Expression For ν

The term ν is the coefficient of $\delta(q)$ in equation (C-25) and is given by,

$$v = \frac{\sigma_j \Delta y_j}{\sqrt{2\pi} (2)} \left[\frac{(y'^2 - z^2)}{(y'^2 + z^2)} + \frac{(y''^2 - z^2)}{(y''^2 + z^2)} \right] \quad (D-41)$$

In the above equation, all terms are constant except z . Since z is a function of n , we can write,

$$v = v(n) \quad (D-42)$$

We can express the values of v for all the wall elements by the matrix $\{v\}$. Where,

$$\{v\} = \begin{bmatrix} v_{11} \\ v_{21} \\ \vdots \\ v_{k21} \end{bmatrix} \quad (D-43)$$

Matrix Expression For $(C_1 + C_2)$

Equation (C-16) and equation (C-17) give the expressions for C_1 and C_2 respectively. If ψ represents the summation of C_1 and C_2 then,

$$\psi = \frac{\sigma_j \Delta y_j z}{2\sqrt{2\pi} (y'^2 + z^2)} + \frac{\sigma_j \Delta y_j z}{2\sqrt{2\pi} (y''^2 + z^2)} \quad (D-44)$$

The above equation can be expressed as a function of z . Since z is a function of n , we can write,

$$\psi = \psi(n) \quad (D-45)$$

The function $\psi(n)$ has a different value for each wall element. For all the K_2 elements we can represent the values of $\psi(n)$ by a column matrix, $\{\psi\}$, of the order $(K_2 \times 1)$.

$$\{\psi\} = \begin{bmatrix} \psi_{11} \\ \psi_{21} \\ \vdots \\ \psi_{K_2 1} \end{bmatrix} \quad (D-46)$$

Matrix Expression For \mathcal{Q}

The term \mathcal{Q} is the coefficient of $\delta(q)$ in equation (C-22).

That is,

$$\mathcal{Q} = \frac{-\gamma_j \Delta y_j z 2 y'}{2 \sqrt{2\pi} (y'^2 + z^2)^2} - \frac{+\gamma_j \Delta y_j z 2 y''}{2 \sqrt{2\pi} (y''^2 + z^2)^2} \quad (D-47)$$

The above equation indicates that \mathcal{Q} is a function of z . All other terms in equation (D-47) are constant. Since the value of z changes for each element on the wall, \mathcal{Q} can be expressed by a column matrix, $\{\mathcal{Q}\}$, of the order $(K_2 \times 1)$.

$$\{\mathcal{Q}\} = \begin{bmatrix} \mathcal{Q}_{11} \\ \mathcal{Q}_{21} \\ \vdots \\ \mathcal{Q}_{K_2 1} \end{bmatrix} \quad (D-48)$$

Matrix Expression For The Influence Coefficient

The influence coefficient, σ , has a different value for each wall element. Hence the values of the influence coefficient for all the k_2 wall elements can be expressed by a matrix $\{\sigma\}$.

$$\{\sigma\} = \begin{bmatrix} \sigma_1 \\ \sigma_2 \\ \vdots \\ \sigma_{k_2} \end{bmatrix} \quad (D-49)$$

The influence coefficient for each element in the above equation has a real part, σ' , and an imaginary part, σ'' .

2. Tranter, C.J. *Bessel Functions With Some Physical Applications*. The English University Press, London, 1969.
3. Baldwin, B.S.; Turner, J.B. and Heckel, E.B. "Wall Interference in Windtunnels with Slotted and Porous Boundaries at Subsonic Speeds", *NACA TR 5316*, May 1954.
4. Davis, D. and Moore, T. "Analytical Study of Blockage and Lift Interference Corrections for Slotted Tunnels Obtained by the Substitution of Equivalent Homogeneous Boundaries in the Discrete Slotted Wall", *NACA TR 5317*, June 1953.
5. Kraft, E.H. "Upwash Interference On a Symmetrical Wing in a Rectangular Ventilated Wall Wind Tunnel", Master's Thesis, University of Tennessee, Knoxville, TN, October 1972.
7. Needer, P.F. "Theoretical Investigation of Supersonic Wall Interference in Rectangular Slotted Test Section", Drown University, Div. of Engineering, Tech Report W-7-11, September 1953.
8. Monti, S. "Wall Corrections for Airplanes with Lift in Irrotational Wind Tunnel Tests", Prepared at request of Fluid Dynamics Panel of AGARD, 1971.
9. Pindzola, M. and Lo, C.F. "Boundary Interference at Subsonic Speeds in Wind Tunnels with Ventilated Walls", AEDC - TR - 69 - 47 (AD687440), May 1969.
10. Vidal, R.J.; Erickson, J.C., Jr. and Catlin, P.A. "Experiments with a Self-Correcting Windtunnel", AGARD CP 134, Wind Tunnel Design and Testing Techniques, October 1975.
11. Wood, W.H. "Tunnel Interference from Slotted Walls", *Quart. J. Mech. Appl. Math.*, Vol. 17, pt. 2, May 1964, pp. 125.
12. Wright, Ray H and Barger, Raymond L. "Windtunnel Lift Interference on Sweptback Wings in Rectangular Test Sections with Slotted Wall and Bottom Walls", NASA TR - 241, June 1959.

BIBLIOGRAPHY

1. Muskat, M. The Flow of Homogeneous Fluids Through Porous Media. McGraw Hill, New York, 1937. pp. 55-120
2. Tranter, C.J. Bessel Functions With Some Physical Applications. The English Universities Press, London, 1968.
3. Baldwin, B.S.; Turner, J.B. and Knechtel, E.D. "Wall Interference in Windtunnels with Slotted and Porous Boundaries at Subsonic Speeds", NACA TN3716, May 1954.
4. Davis, D. and Moore, D. "Analytical Study of Blockage and Lift Interference Corrections for Slotted Tunnels Obtained by the Substitution of an Equivalent Homogeneous Boundary for the Discrete Slots", NACA RM53E07B, June 1953.
5. Holder, D.R. "Upwash Interference On Wings of Finite Span in a Rectangular Windtunnel with Closed Side Walls and Porous Slotted Floor and Roof", ARC R and M 3395, November 1965.
6. Kraft, E.M. "Upwash Interference On a Symmetrical Wing in a Rectangular Ventilated Wall Windtunnel". Master's Thesis, University of Tennessee, Knoxville, TN. October 1972.
7. Maeder, P.F. "Theoretical Investigation of Subsonic Wall Interference in Rectangular Slotted Test Section". Brown University, Div. of Engineering, Tech Report W T - 11. September 1953.
8. Monti, R. "Wall Corrections for Airplanes With Lift in Transonic Wind Tunnel Tests". Prepared at request of Fluid Dynamics Panel of AGARD. 1971.
9. Pindzola, M. and Lo, C.F. "Boundary Interference at Subsonic Speeds in Wind Tunnels with Ventilated Walls". AEDC - TR - 69 - 47 (AD687440). May 1969.
10. Vidal, R.J.; Erickson, J.C., Jr. and Catlin, P.A. "Experiments with a Self-Correcting Windtunnel". AGARD CP 174, Wind Tunnel Design and Testing Techniques. October 1975.
11. Wood, W.W. "Tunnel Interference from Slotted Walls". Quart. J. Mech. Appl. Math., Vol. 17, pt. 2, May 1964. pp. 125
12. Wright, Ray H and Barger, Raymond L. "Windtunnel Lift Interference on Sweptback Wings in Rectangular Test Sections with Slotted Wall and Bottom Walls". NASA TR - 241. June 1966.